MICROCOPY RESOLUTION TEST CHART

NATIONAL BUREAU OF STA...

ETL-0197

LEVEL

Materials research for
holographic recording
(Report No.3, Hardened gelatin
holographic recording materials)

James W. Gladden

John W. Eastes

A076203

SEPTEMBER 1979

DDC
NOV 7 1979

U.S. ARMY CORPS OF ENGINEERS

ENGINEER TOPOGRAPHIC LABORATORIES

FORT BELVOIR, VIRGINIA 22060

79 11 05 127

REPORT DOCUMENTATION PAGE

READ INSTRUCTIONS BEFORE COMPLETING FORM

1. REPORT NUMBER	2. GOVT ACCESSION NO.	3. RECIPIENT'S CATALOG NUMBER
ETL — 0197		

4. TITLE (and Subtitle)

MATERIALS RESEARCH FOR HOLOGRAPHIC RECORDING, HARDENED GELATIN HOLOGRAPHIC RECORDING MATERIALS.

5. TYPE OF REPORT & PERIOD COVERED

Report Number 3.
Technical Report

6. PERFORMING ORG. REPORT NUMBER

7. AUTHOR(s)	8. CONTRACT OR GRANT NUMBER(s)
James W. Gladden John W. Eastes	Technical rept.

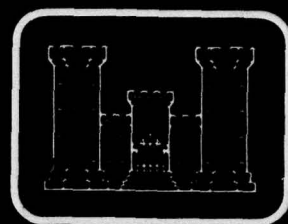**9. PERFORMING ORGANIZATION NAME AND ADDRESS**

U. S. Army Engineer Topographic Laboratories
Fort Belvoir, Virginia   22060

10. PROGRAM ELEMENT, PROJECT, TASK AREA & WORK UNIT NUMBERS

4A161102B52C

11. CONTROLLING OFFICE NAME AND ADDRESS

U. S. Army Engineer Topographic Laboratories
Fort Belvoir, Virginia   22060

12. REPORT DATE

September 1979

13. NUMBER OF PAGES

65

14. MONITORING AGENCY NAME & ADDRESS(if different from Controlling Office)

15. SECURITY CLASS. (of this report)

Unclassified

15a. DECLASSIFICATION/DOWNGRADING SCHEDULE

16. DISTRIBUTION STATEMENT (of this Report)

Approved for public release; distribution unlimited.

17. DISTRIBUTION STATEMENT (of the abstract entered in Block 20, if different from Report)

18. SUPPLEMENTARY NOTES

19. KEY WORDS (Continue on reverse side if necessary and identify by block number)

Diazo	Photosensitive Materials
Diazo Gelatin	Silver Halide (Sensitized) Gelatin
Dichromated Gelatin	
Holography	
Holographic Recording Materials	

20. ABSTRACT (Continue on reverse side if necessary and identify by block number)

The results of a study of four different hardened gelatin holographic recording materials are reported. These are the dichromated, diazo, diazo resin, and silver halide (sensitized) gelatins. The report concludes that of the four photosensitive processes studied, the silver halide (sensitized) gelatin process offers the most promising process characteristics.

The silver halide gelatin process is a new holographic recording process that can be used to prepare phase volume holograms in hardened gelatin.

DD FORM 1473 1 JAN 73   EDITION OF 1 NOV 65 IS OBSOLETE

20. Cont'd

The process uses a reversal bleach that dissolves the developed silver metal image while further crosslinking the gelatin in the vicinity of the silver image. Upon fixing and with dehydration of the resulting gelatin hologram, one obtains recordings similar to those produced by the dichromated gelatin process. This is accomplish with exposures on the order of 200 to 500 $\mu J/cm^2$ at 514.5 nm in a silver halide emulsion that has a panchromatic response. Furthermore, because the hologram has no silver halide present, the hologram does not exhibit the printout phenomena characteristic of bleached holograms.

PREFACE

This work was authorized by the U. S. Army Engineer Topographic Laboratories (ETL), Fort Belvoir, Virginia under DA Project 4A161102B52C entitled "Research in Geodetic, Cartographic, and Geographic Sciences."

The results of a study of four different hardened gelatin holographic recording materials are reported. These are the dichromated, diazo, diazo resin, and silver halide (sensitized) gelatins. The report concludes that of the four photosensitive processes studied, the silver halide (sensitized) gelatin process offers the most promising process characteristics.

The authors would like to thank Mr. William R. Graver, Research Institute, ETL* who designed and erected the optical arrangements shown in Schemes 2 and 3 of this report. We wish to acknowledge the many discussions with Mr. Graver during the course of this work. Mr. Michael M. McDonnell, Research Institute, ETL, was also an interested contributor to this work. He was instrumental in preparing the first holograms including a reflection hologram using the new silver halide (sensitized) gelatin process described in this report. His efforts are appreciated.

COL Daniel L. Lycan, CE, was Commander and Director of ETL during the report preparation. Mr. Robert P. Macchia was the Technical Director.

*Mr. Graver is now with Riverside Research Institute, Arlington, Virginia.

CONTENTS

2

CONTENTS Cont'd

TABLES

ILLUSTRATIONS

ILLUSTRATIONS Cont'd

5

MATERIALS RESEARCH FOR HOLOGRAPHIC RECORDING
(REPORT NO. 3, HARDENED GELATIN HOLOGRAPHIC RECORDING MATERIALS)

INTRODUCTION

PURPOSE ■ Since 1970, the U. S. Army Engineer Topographic Laboratories (ETL) has supported research in coherent optics applied to mapping. Because one aspect of this research is to evaluate photosensitive recording materials with potential applications in holographic storage and other coherent optical systems, ETL has developed an extensive testing facility for parametric studies of materials deemed suitable for holographic recording. Earlier reports in this series treated the storage of continuous tone data in volume holograms and bleaching techniques for silver halide holograms.[1,2] The present report describes work and results obtained with a variety of hardened sensitized gelatins.

Although considerable work has been carried out by others with dichromated gelatin (DCG) as a recording material, it will be included in this study.[3,4,5] In addition to DCG, alternative gelatins, such as diazo (sensitized) gelatin (DAG), diazo resin (sensitized) gelatin (DRG), and a new silver halide (sensitized) gelatin (SHG) are described.

Our interest in studying gelatin processes is that gelatin possesses almost ideal properties for phase holograms. When properly used, it forms a clear film that exhibits very little absorption and optical scattering.

---

[1] John W. Eastes, *Material Research for Holographic Recording (Report No. 1, Multiple Image Storage of Continuous Tone Data in Volume Holograms)*. U. S. Army Engineer Topographic Laboratories, Fort Belvoir, VA, ETL--0088 July 1976, NTIS: AD-A035 457.

[2] John W. Eastes, *Materials Research for Holographic Recording (Report No. 2, Bleaching Methods for Photographically Recorded Holograms)*, U. S. Army Engineer Topographic Laboratories, Fort Belvoir, VA, ETL--0156, August 1978, NTIS: AD-A059 548.

[3] T. A. Shankoff, "Phase Holograms in Dichromated Gelatin," *Applied Optics*, Vol. 7, No. 10, pp 2101-2105, Oct 1968.

[4] L. H. Lin, "Hologram Formation in Hardened Dichromated Gelatin Films," *Applied Optics*, Vol. 8, No. 5, pp 963-966, May 1969.

[5] Dietrich Meyerhofer, "Spatial Resolution of Relief Holograms in Dichromated Gelatin," *Applied Optics*, Vol. 10, No. 2, pp 416-21, February 1971.

SCOPE ■ The report describes four different photosensitive materials, referred to as hardened gelatin holographic recording materials, which offer some potential for off–axis holography. The report consists of an introduction, a description of the optical arrangements, a section on gelatin, a description of the four recording materials, a discussion, the conclusions, and a section entitled future studies. The DAG, DRG, and SHG processes are described in detail, including process mechanisms, chemistry, preparation methods and their characteristic exposure curves. However, a general treatment is given to the DCG process because of the large body of literature that exists on it. The four processes are compared and contrasted in the discussion, and an analysis is made of their suitability for off–axis holography.

BACKGROUND ■ This section describes fundamentals used in the report. That UV and VIS light can produce chemical changes or photolysis in certain materials has been known for many years. Photochemical reactions involve electronic transitions in molecules, and nearly all those electronic transitions occur in the ultraviolet and visible region of the electromagnetic spectrum. The Grotthus–Draper law states that only radiation that is absorbed by the molecules can cause photochemical reactions. Not all radiation that is absorbed produces photochemical reactions, but photochemical reactions can only occur when radiation is absorbed. The extent to which radiation is absorbed by different materials is determined with techniques in absorption spectroscopy.

Silver halide materials are unique among photosensitives materials in that the photosensitive unit is a silver halide crystallite, that is, a minute crystal. A silver bromide crystallite that has a volume of 10^{-12} cubic millimeters is composed of about 8.3×10^7 molecules. This would be a crystallite in a fine–grained emulsion. The absorption of 4 to 25 quanta per crystallite results in conversion of the entire crystallite during development into a grain of metallic silver, which is the basic imaging unit. The conversion is accomplished with very large quantum yield, and it is this property of silver halide materials that produces their very high sensitivity. Upon photolysis, most photosensitive materials produce image units having molecular dimensions. Other materials may produce image units comprised of hundreds to thousands of molecules with the absorption of a single quantum of actinic radiation. Although these photosensitive materials do not exhibit the photosensitivity of the silver halide materials, they may have higher recording resolutions than the silver halides that typically have larger image units.

7

High resolution is a required feature for recording materials used in off-axis holography. The recorded spatial frequency is dependent upon (1) the angle between the two coherent beams of light at the recording plane (scheme 1) and (2) the wavelength. If the bisector of the angle that the two beams make in air is normal to the recording plane, then one-half of the interbeam angle is defined as θ_a. The spatial frequency, ν, may be calculated from the following relationship:

$$\nu = \frac{1}{d} = 2 \frac{Sin\theta_a}{\lambda_a}$$

in which d is the distance between corresponding regions in the interference pattern, and λ_a is the wavelength of the coherent light in air. Because of refraction that occurs as the light enters the recording medium, θ_a and λ_a become θ_m and λ_m. Then, with Snell's Law

$$\frac{Sin\theta_a}{\lambda_a} = \frac{Sin\theta_m}{\lambda_m} \quad \text{and} \quad \nu = 2 \frac{Sin\theta_m}{\lambda_m}$$

Thus, the spatial frequency is the same in both air and the recording medium. If θ_a = 30 degrees and λ_a = 0.633 x 10^{-3} millimeters for the red line of the helium neon laser, the spatial frequency is 1,580 c/mm (cycles per millimeter). As θ_a increases or the wavelength of the coherent light decreases, the resulting spatial frequencies increase. Spatial frequencies approaching 4,000 c/mm have been recorded.

The photosensitive processes described in this report are classified in three catagories. The first consists of those processes that form patterns of low $\Delta\eta$* during exposure. These semi-self-developing materials include the DCG, DAG, and DRG processes. The second catagory includes the SHG process that forms a latent image during exposure. Both catagories of materials form patterns of high $\Delta\eta$ upon processing. A third catagory of materials forms patterns of high $\Delta\eta$ during exposure. These materials are totally self-developing, and they form distortions in their refractive index patterns by a process that does not appear to be in accord with Snell's Law.

*$\Delta\eta$ is defined as the refractive index difference between image and non-image area.

8

Beam Splitter

Mirror

Recording Plane

Laser
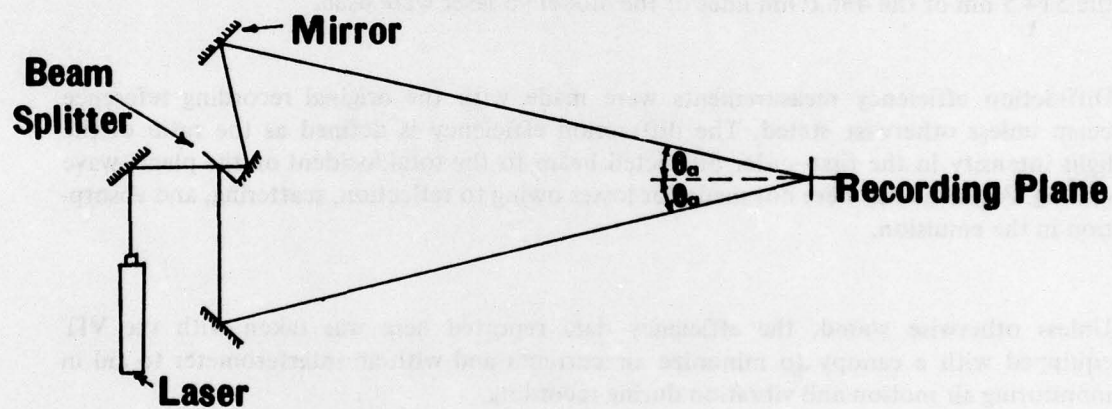
**SCHEME 1.   Holographic Optical Arrangements**

9

OPTICAL ARRANGEMENTS

Two recording schemes were optically arranged on a 4-by 8-foot vibration isolating table (VIT) manufactured by Newport Research Corporation (NRC). In scheme 2, the Spectra Physics Model 125 He-Ne laser with Model 250 excitor is used. The Model 125 laser is mounted beneath the table, and the beam is directed to the table top by the NRC's Model 650 beam-steering instrument. In scheme 3, the Lexel Model 95 argon ion laser with a 35 ampere power supply is used, equipped with the optional laser power meter, the light regulator control and control selector, and the optional range selector. Also, the laser head is equipped with an etalon and thermostated oven. The Model 95 laser is mounted on top of the VIT, and the beam is elevated to 10 inches (25 cm) above and level with the table top with the aid of NRC's Model 670 beam-steering instrument. Scheme 2 was used only in some initial work with the SHG process; Scheme 3, was used for the bulk of the work with SHG, DCG, DAG, and DRG processes. In scheme 3, either the 514.5 nm or the 488.0 nm lines of the Model 95 laser were used.

Diffraction efficiency measurements were made with the original recording reference beam unless otherwise stated. The diffraction efficiency is defined as the ratio of the light intensity in the first-order diffracted beam to the total incident on the plane-wave grating. Adjustments were not made for losses owing to reflection, scattering, and absorption in the emulsion.

Unless otherwise stated, the efficiency data reported here was taken with the VIT equipped with a canopy to minimize air currents and with an interferometer to aid in monitoring air motion and vibration during recording.

A time period was observed between movements of the plate holder and before starting an exposure to insure that there was no residual motion between the interference pattern being recorded and the sensitized gelatin plate during recording.
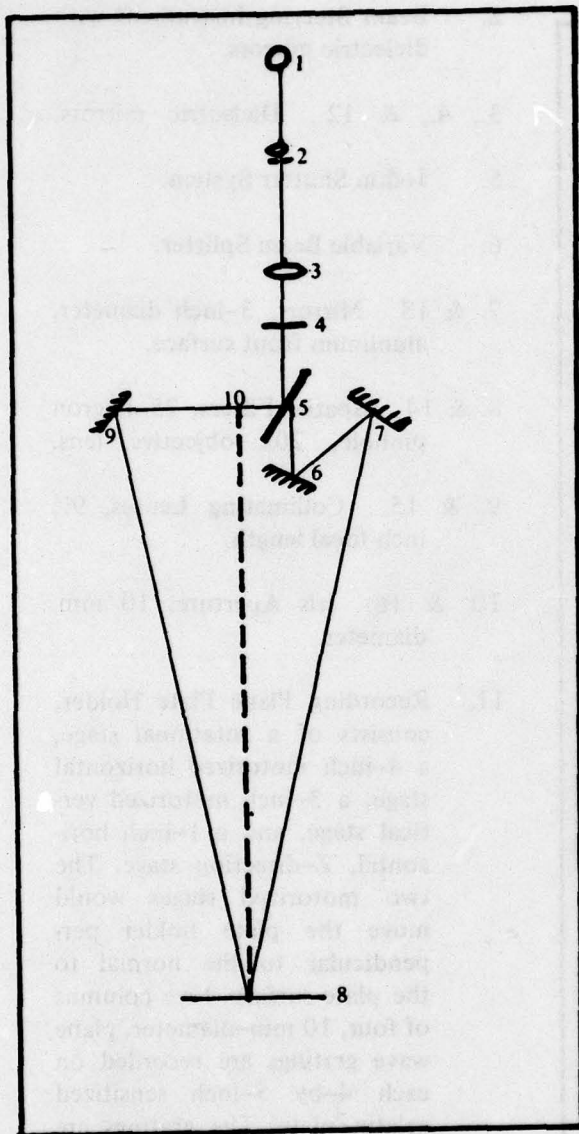
1. Beam Steering Instrument.

2. Spatial Filter, 25–micron pin-hole, 40x objective lens.

3. Collimating lens, 5–inch focal length, 1–inch diameter, achromatic.

4. Iris Aperture, less than 1–inch diameter.

5. Beam Splitter, 4–inch diameter.

6. 7., & 9. MIRRORS, 3–inch diameter, aluminum front surface.

8. Recording Plane Plate Holder, consists of a rotational stage and 4–inch travel translational stage. The rotational stage is mounted on a jack, and the 4-by 5–inch plate holder is mounted atop the translational stage.

10. This point is equi–distant between points 7 and 9.

The Distance 5 to 6 to 7 = 5 to 10 to 9. The Distance 7 to 8 = 8 to 9.
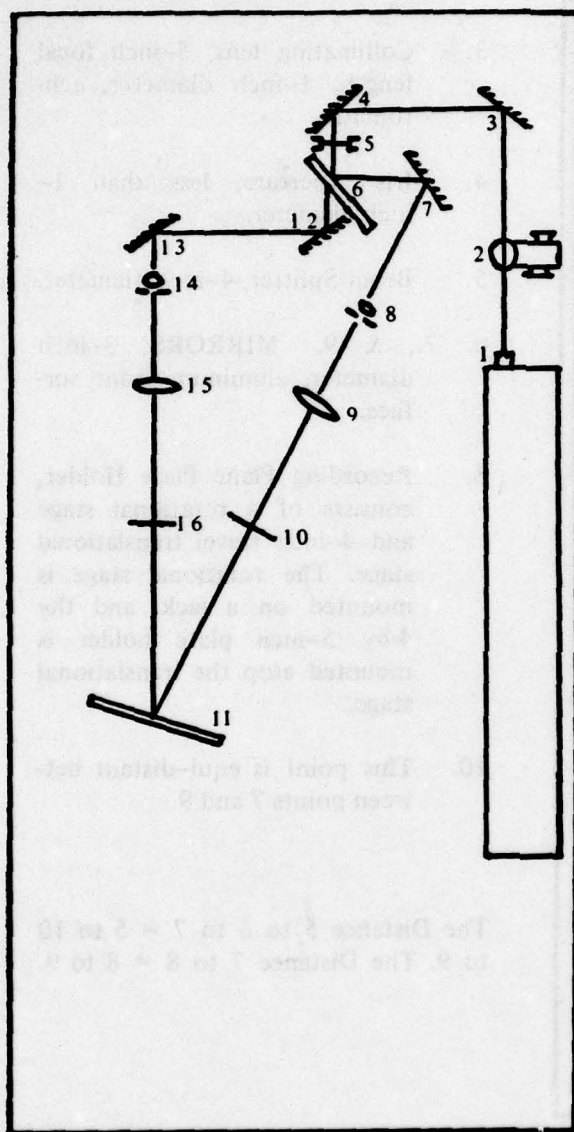
SCHEME 2.   He–Ne Laser

1. Lexel Model 95 Argon Ion Laser.

2. Beam Steering Instrument with dielectric mirrors.

3., 4., & 12. Dielectric mirrors.

5. Jodon Shutter System.

6. Variable Beam Splitter.

7. & 13 Mirrors, 3–inch diameter, aluminum front surface.

8. & 14 Spatial Filters, 25–micron pinhole, 20x objective lens.

9. & 15. Collimating Lenses, 9½ inch focal length.

10. & 16. Iris Aperture, 10 mm. diameter.

11. Recording Plane Plate Holder, consists of a rotational stage, a 4–inch motorized horizontal stage, a 3–inch motorized vertical stage, and a 1–inch horizontal, Z–direction stage. The two motorized stages would move the plate holder perpendicular to the normal to the plate surface. Five columns of four, 10 mm–diameter, plane wave gratings are recorded on each 4–by 5–inch sensitized gelatin plate. The gratings are on approximately 22 mm centers.

SCHEME 3. Argon Ion Laser

GELATIN

BACKGROUND ▪ Gelatin is prepared from collagen, which is a fibrous protein found in certain animal tissue, such as skin, tendons, ligaments, bones, etc. In collagen, three polymer chains are twisted around one another to form a three–stranded helix. The gelatin is prepared by separating the strands of the collagen helix and thus converting it to this water–soluble protein. This is accomplished by boiling the collagen containing animal tissue in water. Upon cooling, the dispersion of gelatin in water does not revert to collagen, but sets to a gel. The gelatin has a molecular weight approximately one–third of that of the collagen. Mees and James[6] state that most photographic gelatins are prepared by treating collagen stock with a lime slurry at 10 to 20°C for weeks, or even months. The stock is then washed and neutralized with acid. The gelatin is extracted with warm water at neutral or slightly acid pH in a series of "cooks," each at successively more elevated temperatures. The resultant gelatin dispersions are filtered, clarified, concentrated, cooled, allowed to gel, and then dried.

To understand the chemical structure of gelatin, one must consider its amino acids. Chemically, gelatin is a polymer, consisting of monomeric α–amino acids. A single gelatin molecule may contain more than 2,000 amino acid units, and there can be 19 or more different units in each molecule. Thus, the number of different possible combinations of units is almost infinite.

In table 1, the 19 natural amino acids are compiled that are found in most photographic gelatin. Missing in the table are asparagine and glutamine, which are found in collagen. These amino acids are hydrolyzed to aspartic acid and glutamic acid units during the liming process. An approximate amino acid content of a gelatin is taken from *The Merck Index*[7] and compiled in table 2. From this, a molecular formula may be calculated as shown in the table. The total number of amino acid units in the gelatin molecule is seen to be 2,431, and the molecular weight of the gelatin is approximately 220,000. The total percent composition is greater than 100 percent because water is incorporated in the molecules of the individual amino acids.

---

[6] C. E. Kenneth Mees and T. H. James, Editors, *The Theory of the Photographic Process*, 3rd Ed., 1966, The Macmilliam Co., New York, p. 46.

[7] Paul G. Stecher, Editor, *The Merck Index*, 8th Ed., 1968, Merck & Co., Inc., Rahway, NJ, p. 484.

From table 1, we see that the formula,

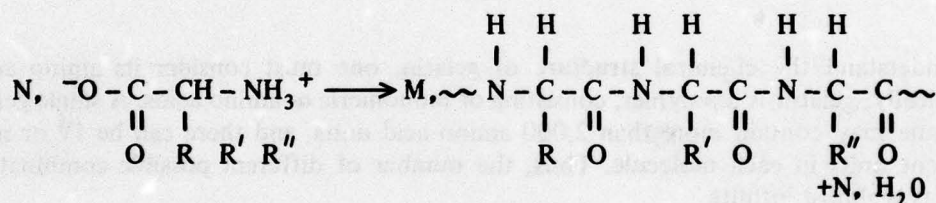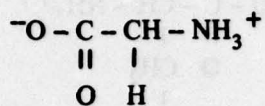$$\text{}^-O - \underset{\underset{O}{\|}}{C} - \underset{\underset{R}{|}}{CH} - NH_3{}^+$$
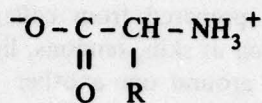
is common to 15 of the listed amino acids. From this chemical feature, the amino acids form the long chain polyamides that make up the gelatin molecule. Thus, we have

$$N, \; {}^-O - \underset{\underset{O}{\|}}{C} - \underset{\underset{R}{|}}{CH} - \underset{\underset{R'}{|}}{N}H_3{}^+ \longrightarrow M, \sim N - \underset{\underset{R}{|}}{\overset{\overset{H}{|}}{C}} - \underset{\underset{O}{\|}}{\overset{\overset{H}{|}}{C}} - N - \underset{\underset{R'}{|}}{\overset{\overset{H}{|}}{C}} - \underset{\underset{O}{\|}}{\overset{\overset{H}{|}}{C}} - N - \underset{\underset{R''}{|}}{\overset{\overset{H}{|}}{C}} - \underset{\underset{O}{\|}}{\overset{\overset{H}{|}}{C}} \sim$$
$$+N, \; H_2O$$

in which every third atom of the polyamide chain is attached to a side chain denoted by R, R′, and R″. The structure depends upon the particular amino acid unit involved (e.g. R may be –H for glycine, R′ may be $-CH_2CH_2CH_2CH_2NH_3{}^+$ for lysine, and R″ may be $-CH_2COOH$ for aspartic acid). This may be written in the form Gly.Lys.Asp. to denote the order of glycine, lysine, and aspartic acid in the trimer. In table 2, notice that gelatin is characterized by a high proportion of proline and hydroxyproline amino acid units. Gelatin is also characterized by frequent repetitions of the sequence Gly.Pro.Hypro., which can comprise almost one–third of the molecule. The glycine unit appears to be uniformly distributed throughout the gelatin molecule. But, those regions of the gelatin molecule rich in proline and hydroxyproline units are deficient in the more polar units, such as lysine, arginine, and aspartic and glutamic acids, and vice versa. Thus, we see that the long chain gelatin molecule is made up of alternating regions of a polar and nonpolar character.

14

TABLE 1.   NATURAL AMINO ACIDS

$^-O - C - CH - NH_3^+$
$|| \quad |$
$O \quad H$

Glycine (Gly)
M.W.: 75.07

$^-O - C - CH - NH_3^+$
$|| \quad |$
$O \quad CH_3$

Alanine (Ala)
M.W.: 89.09

$^-O - C - CH - NH_3^+$
$|| \quad |$
$O \quad CH_2$
$\quad \quad |$
$\quad \quad OH$
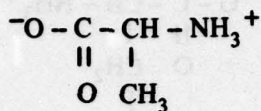
Serine (Ser)
M.W.: 105.09

$^-O - C - CH - NH_3^+$
$|| \quad |$
$O \quad CH_2$
$\quad \quad |$
$\quad \quad SH$

Cysteine (CySH)
M.W.: 121.16

$^-O - C - CH - NH_3^+$
$|| \quad |$
$O \quad CH_2$
$\quad \quad |$
$\quad \quad S$
$\quad \quad |$
$\quad \quad S$
$\quad \quad |$
$O \quad CH_2$
$|| \quad |$
$^-O - C - CH - NH_3^+$
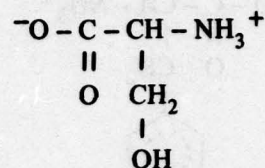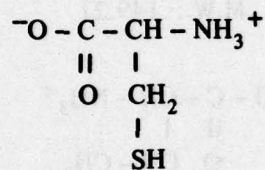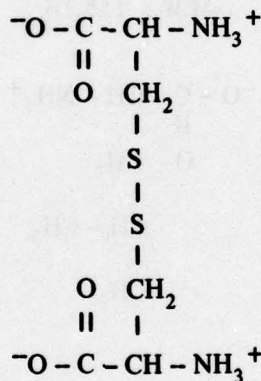
Cystine (CyS – SCy)
M.W.: 240.30

$^-O - C - CH - NH_3^+$
$|| \quad |$
$O \quad CH_2$
$\quad \quad |$
$\quad \quad C = 0$
$\quad \quad |$
$\quad \quad OH$
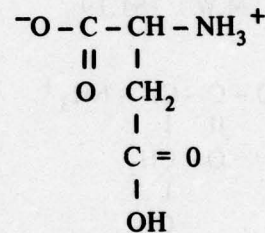
Aspartic Acid (Asp)
M.W.: 133.10

$^-O - C - CH - NH_3^+$
$|| \quad |$
$O \quad CH - CH_3$
$\quad \quad |$
$\quad \quad CH_3$

Valine (Val)
M.W.: 117.15

$^-O - C - CH - NH_3^+$
$|| \quad |$
$O \quad CHOH$
$\quad \quad |$
$\quad \quad CH_3$
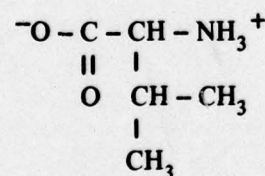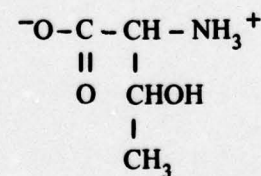
Threonine (Thr)
M.W.: 119.12

$^-O - C - CH - NH_3^+$
$|| \quad |$
$O \quad CH_2$
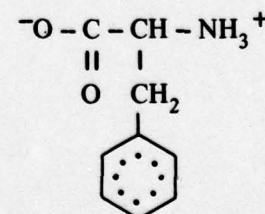
Phenylalanine (Phe)
M.W.: 165.19

15

TABLE 1. Continued

$$^-O-C-CH-NH_3^+$$
$$\quad\ \|\quad\ |$$
$$\quad\ O\quad CH_2$$

(phenol ring with OH)

Tyrosine (Tyr)
M.W.: 181.19

$$^-O-C-CH-NH_3^+$$
$$\quad\ \|\quad\ |$$
$$\quad\ O\quad CH_2$$

(imidazole ring, NH, N)
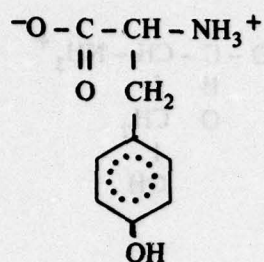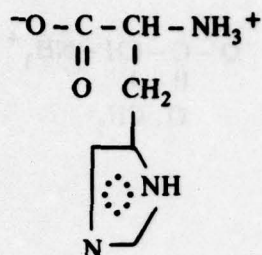
Histidine (His)
M.W.: 155.16

$$^-O-C-CH-NH_3^+$$
$$\quad\ \|\quad\ |$$
$$\quad\ O\quad CH_2$$
$$\qquad\quad\ |$$
$$\qquad\quad CH_2$$
$$\qquad\quad\ |$$
$$\qquad\quad\ S$$
$$\qquad\quad\ |$$
$$\qquad\quad CH_3$$
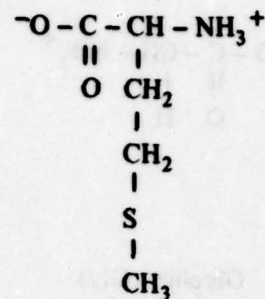
Methionine (Met)
M.W.: 149.21

$$^-O-C-CH-NH_3^+$$
$$\quad\ \|\quad\ |$$
$$\quad\ O\quad CH_2$$
$$\qquad\quad\ |$$
$$\qquad\quad CH_2$$
$$\qquad\quad\ |$$
$$\qquad\quad C=O$$
$$\qquad\quad\ |$$
$$\qquad\quad OH$$
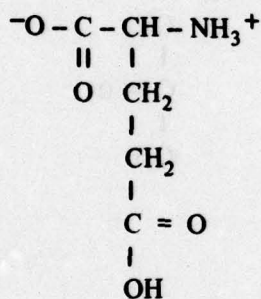
Glutamic Acid (Glu)
M.W.: 147.13

$$^-O-C-CH-NH_3^+$$
$$\quad\ \|\quad\ |$$
$$\quad\ O\quad CH_2$$
$$\qquad\quad\ |$$
$$\qquad\quad CH-CH_3$$
$$\qquad\quad\ |$$
$$\qquad\quad CH_3$$
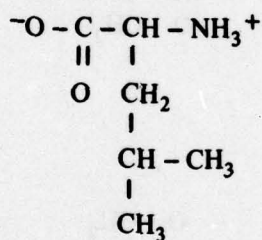
Leucine (Leu)
M.W.: 131.17

$$^-O-C-CH-NH_3^+$$
$$\quad\ \|\quad\ |$$
$$\quad\ O\quad CH-CH_3$$
$$\qquad\qquad\ |$$
$$\qquad\qquad CH_2$$
$$\qquad\qquad\ |$$
$$\qquad\qquad CH_3$$
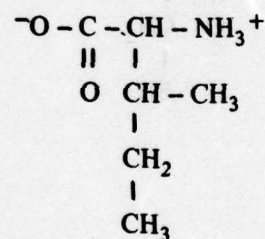
Isoleucine (Ileu)
M.W.: 131.17

1 6

TABLE 1. Continued

$$^-O - C - CH - NH_2$$
$$\qquad \| \quad \; |$$
$$\qquad O \quad CH_2$$
$$\qquad \qquad |$$
$$\qquad \qquad CH_2$$
$$\qquad \qquad |$$
$$\qquad \qquad CH_2$$
$$\qquad \qquad |$$
$$\qquad \qquad CH_2$$
$$\qquad \qquad |$$
$$\qquad \qquad +NH_3$$

Lysine (Lys)
M.W.: 146.19

$$^-O - C - CH - NH_2$$
$$\qquad \| \quad \; |$$
$$\qquad O \quad CH_2$$
$$\qquad \qquad |$$
$$\qquad \qquad CH_2$$
$$\qquad \qquad |$$
$$\qquad \qquad CH_2$$
$$\qquad \qquad |$$
$$\qquad \qquad NH$$
$$\qquad \qquad |$$
$$\qquad \qquad C = N^+H_2$$
$$\qquad \qquad |$$
$$\qquad \qquad NH_2$$
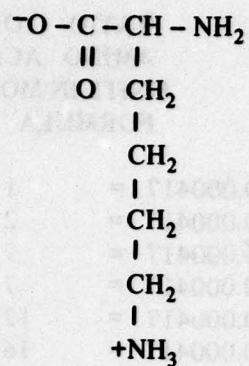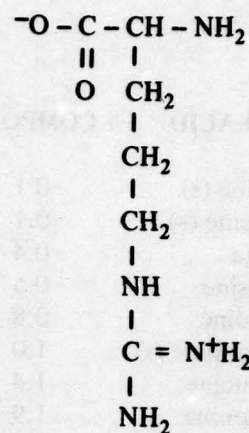
Arginine (Arg)
M.W.: 174.20

$$^-O - C - CH - N^+H_2$$
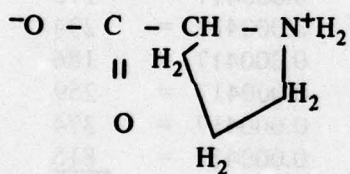
Proline (Pro)
M.W.: 115.13

$$^-O - C - CH - N^+H_2$$
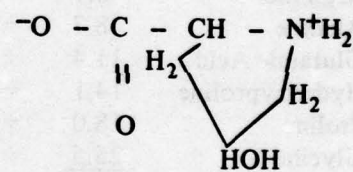
Hydroxyproline (Hypro)
M.W.: 131.13

17

TABLE 2. GELATIN MOLECULAR FORMULA

AMINO ACID	% COMPOSITION		MOL. WT.						RATIO OF AMINO ACID UNITS IN MOL. FORMULA
Cystine (s)	0.1	÷	240	=	0.000417	÷	0.000417	=	1
Cysteine (s)	0.1	÷	121	=	0.000825	÷	0.000417	=	2
Serine	0.4	÷	105	=	0.00381	÷	0.000417	=	9
* Tyrosine	0.5	÷	181	=	0.00277	÷	0.000417	=	7
Histidine	0.8	÷	155	=	0.00517	÷	0.000417	=	12
Methionine (s)	1.0	÷	149	=	0.00670	÷	0.000417	=	16
Isoleucine	1.4	÷	131	=	0.0107	÷	0.000417	=	26
Threonine	1.9	÷	119	=	0.0160	÷	0.000417	=	38
Phenylalanine	2.2	÷	165	=	0.0134	÷	0.000417	=	32
Valine	2.5	÷	117	=	0.0214	÷	0.000417	=	51
Leucine	3.2	÷	131	=	0.0245	÷	0.000417	=	59
* Lysine	4.1	÷	146	=	0.0281	÷	0.000417	=	67
* Aspartic Acid	6.6	÷	133	=	0.0496	÷	0.000417	=	119
* Arginine	8.1	÷	174	=	0.0466	÷	0.000417	=	112
Alanine	8.7	÷	89	=	0.0975	÷	0.000417	=	234
* Glutamic Acid	11.4	÷	147	=	0.0775	÷	0.000417	=	186
Hydroxyproline	14.1	÷	131	=	0.108	÷	0.000417	=	259
Proline	18.0	÷	115	=	0.156	÷	0.000417	=	374
Glycine	25.5	÷	75	=	0.340	÷	0.000417	=	815

TOTALS 110.6%   2431

(s) Denotes sulfur containing amino acids.

* Denotes the polar amino acids.

18

The alternating regions of a polar and nonpolar character on the long gelatin molecule is important to the structure that the gelatin assumes when dried. The gelatin film, dried above its melting point (e.g. 35–45° C), is amorphous; the film dried below the melting point assumes a more crystalline nature. The crystalline regions are produced by the intertwining of three gelatin molecules to form a triple–stranded helix. The helices are produced in the nonpolar regions of the molecule, and the polar sections remain untwined and of a more amorphous character. Diagrams of warm, dried amorphous film and the cool, dried crystalline film are shown in a review article by Jolley.[8]

Gelatin molecules have reactive side groups through which they can be chemically cross-linked. The reactive side groups are found almost entirely in the polar regions of the molecule. For the most part, the amino acids that contain the reactive side groups are lysine, arginine, and aspartic and glutamic acids, which make up one–fifth of the amino acid units in the gelatin molecule described in table 2. Generally, it has been demonstrated that cationic complexes of chromium form crosslinks through coordination with the carboxyl groups of the aspartic and glutamic acids side chains, and crosslinks formed with organic reagents involve the amine group of the lysine side chains. Thus, the addition of chromium alum to solutions of gelatin produces the formation of the structure:

$$
\text{Gel} - \underset{\underset{O}{\|}}{C} - O - \underset{\underset{\underset{HO}{\diagdown}}{\overset{\overset{OH}{\diagup}}{}}}{Cr} - SO_4 - \underset{}{Cr} - O - \underset{\underset{O}{\|}}{C} - \text{Gel} \tag{1}
$$
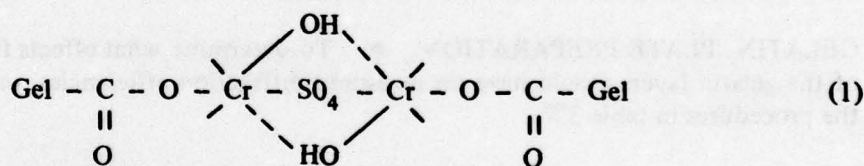
in hardened gelatin.

---

[8] J. E. Jolley, "The Microstructure of Photographic Gelatin Binder," *Photographic Science and Engineering*, Vol. 14, No. 3, May--June 1970, p. 173.

The crosslinks formed upon addition of the organic reagent, p–benzoquinone, is described by the following:

$$\text{[structure with O=C...C=O]} + 2\,H_2N - Gel \longrightarrow Gel - NH \text{[ring with OH, OH]} NH - Gel \qquad (2)$$
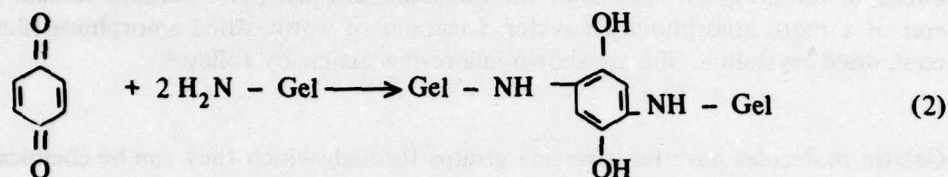
Both crosslinking processes are of interest because structure (1) may be considered representative of that formed in dichromated gelatin and silver halide (sensitized) gelatin processes and because structure (2) may be considered representative of that formed by tanning developers.

GELATIN PLATE PREPARATION ■ To determine what effects further hardening of the gelatin layers would have on measured diffraction efficiencies, one should follow the procedures in table 3.

This is a modified procedure to that offered by W. S. Colburn et al.[9] used to prepare gelatin layers from Kodak 649F plates. Part A of Kodak Rapid Fixer is believed to contain no hardener. The room temperature was between 18 and 22° C. The running water temperature was adjusted to between 20 and 22° C.

[9]W. S. Colburn, R. G. Zech, & L. M. Ralston, *Holographic Optical Elements*, Air Force Avionics Lab, Air Force Systems Command, Wright-Patterson Air Force Base, Ohio, Report No. AFAL--TR--72--409, January. 1973, p. 50.

TABLE 3.   THE HARDENED GELATIN PLATE PREPARATION

	PROCEDURE	TEMP	TIME
1.	Fix in Part A of Kodak Rapid Fixer.	Rm. Temp.	10 mins.
2.	Wash in running water.	20–22° C	15 mins.
3.	Stand in air and drain	Rm. Temp.	1 min.
4.	Rinse in distilled water with 2 drops per liter of Photo-Flow 200.	Rm. Temp.	30 secs.
5.	Dry completely in room air.	Rm. Temp.	≥2 hrs.
6.	Soak in distilled water.	Rm. Temp.	2 mins.
7.	Harden in Parts A & B of Kodak Rapid Fixer.	Rm. Temp.	10 mins.
8.	Wash in running water.	20–22° C	15 mins.
9.	Rinse in distilled water with 2 drops per liter of Photo-Flow 200	Rm. Temp.	30 secs.
10.	Dry completely in room air.	Rm. Temp.	overnight

To study the effects of additional hardening on the efficiency, one should follow the procedures in tables 3 and 4.

TABLE 4.   CONTINUING THE HARDENED GELATIN PLATE PREPARATION

	PROCEDURE	TEMP	TIME
11.	Harden in 0.5% $(NH_4)_2Cr_2O_7$ solution.	Rm. Temp.	5 mins.
12.	Harden in Parts A & B of Kodak Rapid Fixer.	Rm. Temp.	5 mins.
13.	Wash in running water.	20–27° C	15 mins.
14.	Rinse in distilled water with 2 drops per liter of Photo-Flow 200.	Rm. Temp.	30 secs.
15.	Dry completely in room air.	Rm. Temp.	≥2 hrs.

Subsequently the prepared gelatin plates were sensitized in either a 2 percent solution of para-diazodiphenylamine sulfate or a 5 percent solution of ammonium dichromate following the procedure outlined in table 3 and 4. The para-diazodiphenylamine sulfate-sensitized gelatin produced gratings with an efficiency of 6.1 percent at an exposure of 109 mJ/cm^2 (millijoule per square centimeter) using the procedure outlined in table 3. The efficiency was   reduced to less than   0.1 percent at exposures greater than 100

2 1

mJ/cm^2 using the procedure outlined in table 4. The ammonium dichromate sensitized gelatin produced gratings with an efficiency of 66 percent at an exposure of 97 mJ/cm^2 using the procedure outlined in table 3 and with an efficiency of 1.8 percent at an exposure of 249 mJ/cm^2 using the procedure outlined in table 4. The data indicated that the additional hardening of the gelatin, although effective in reducing the amount of precipitated gelatin that appears on the completely processed gelatin plates, reduces the maximum efficiency that can be expected and increases the exposure required to obtain that efficiency. The results demonstrate that the peak efficiency is obtained in gelatin with less chemical hardening. Thus, the procedure outlined in table 5 was employed for the bulk of the work in the DCG, DAG, and DRG processes and was adopted to fix and remove the dye–sensitizer from the Kodak 649F plates. Generally the non–hardening Kodak F–24 Fix may be used when processing solutions and wash waters that do not exceed 18° C, and there is ample drying time so that relatively cool air can be used. We found no difficulty in using this fix in the procedure shown in table 5.

TABLE 5. GELATIN PLATE PREPARATION FOR DCG, DAG, & DRG PROCESSES PROCEDURE

	PROCEDURE	TEMP	TIME
1.	Fix in Kodak Fixer F–24.[a]	Rm. Temp.	10 mins.
2.	Wash in running water.	20–22° C	15 mins.
3.	Stand in air and drain.	Rm. Temp.	1 min.
4.	Rinse in distilled water with 5 drops per liter of Photo-Flow 200.	Rm. Temp.	30 secs.
5.	Dry completely in room air.	Rm. Temp.	≥2 hrs.
6.	Soak in distilled water.	Rm. Temp.	2 mins.
7.	Soak further in Kodak Fixer F–24.	Rm. Temp.	10 mins.
8.	Wash in running water.	20–22° C	15 mins.
9.	Rinse in distilled water with 5 drops of Photo-Flow 200 per liter H_2O.	Rm. Temp.	30 secs.
10.	Dry completely in room air.	Rm. Temp.	overnight

a. Nonhardening Kodak F-24 Fix

Distilled Water (50°C)	500 cc
Sodium Thiosulfate (Hypo)	240.0 grs.
Sodium Sulfite, desiccated	10.0 grs.
Sodium Bisulfite	25.0 grs.
Distilled water to make	1.0 lit.

22

Using the procedure outlined in table 5, one produces a peak efficiency of 68.2 percent at an exposure of 44 mJ/cm^2, which is an exposure less than half of that used for the DCG grating prepared from procedures in table 3. Although the softer gelatin tends to produce the higher efficiency at lower exposure levels, there is the tendency to precipitate more gelatin in the unexposed regions of the gelatin plate upon dehydration in pure isopropanol. The precipitated gelatin appears milky white in the unexposed regions of the gelatin plate. It is not clear whether or not this milky color denotes an increase in scattering in the grating area, which looks comparatively clear in the blue laser light. The milky color disappears by simply wetting the plate in water and then drying it. The milky color appears greater on the DAG processed plates. The difference may be attributed to the dichromate sensitizing solution, somewhat hardening the gelatin plate that is otherwise unaffected by the diazo solution. Finally, the second soak in Kodak Fixer F–24 and wash appears useful in removing the sensitizer dye from the Kodak 649F plate.

DICHROMATED GELATIN

BACKGROUND ■ The distinguishing feature of hardened dichromated gelatin is that thin layers will not dissolve in water, although they will swell to three or four times their dry thickness. In discussing hardening of gelatin and emulsions, Pouradier and Burness point out that (1) the photographic emulsions are hardened during manufacture to protect against the effects of high temperatures and humidities, (2) the emulsions may be hardened during processing to keep the wet gelatin firm and abrasion resistant, and (3) the gelatin may be further hardened through photochemical processes that produce inorganic or organic hardeners as photolysis products.[10] Inorganic hardeners include chromium salts, aluminum salts, and potassium and ammonium alums. Organic hardeners include the chemical families of aldehydes, ketones, acids, and others that augment hardening of the gelatin by forming strong hydrogen bonds, such as afforded by alcohol, phenols, or amines. As there are many different hardeners, so are there a number of different sites in the gelatin molecule through which the hardeners crosslink the gelatin chains. Thus, the degree of crosslinking is important to the hardened dichromated gelatin process.

---

[10]J. Pouradier, and D. M. Burness, "The Hardening of Gelatins and Emulsions," in T. H. James (Ed.) *The Theory of the Photographic Process*, New York, Macmillan Co., 1966, pp 54--60.

Graube describes two basic theories in which image formation may occur, (1) the crack or void, theory and (2) the small aggregate theory.[11] In the crack theory, which is treated in some detail by Curran and Shankoff,[12] a series of cracks is assumed to be formed between highly exposed fringe planes in the gelatin during rapid dehydration of the exposed gelatin emulsion in a warm alcohol bath. In the small aggregate theory, the image—forming mechanism is either the formation of specific chemical compounds, e.g. the chromium III — isopropyl alcohol complex reported by Meyerhofer,[13] or the formation of vacuoles or micro—pores smaller than the wavelength of light.

Probably each process is partially correct and applies to some extent, depending on the exposing and processing conditions of the plate.

SENSITIZATION AND PROCESSING PROCEDURES ▪ The following procedure was used to sensitize and process the dichromated gelatin plates. The sensitization follows the gelatin plate preparation shown in table 5. Data were taken both with and without use of canopy to minimize air currents as indicated. Exposure was at 488.0 nm (nano-meters). We selected this wave length rather than the 514.5 nm line used by most re-searchers because there is greater absorption at 488.0 nm than at 514.5 nm; hence, there should be greater spectral sensitivity at the shorter wave length.

[11]Andrejs Graube, *Holographic Optical Element Materials Research*, Hughes Research Laboratories, Malibu, CA. AFSC Contract F44620--76--0064, March 1977, p 25.

[12]R. K. Curran and T. A. Shankoff, "The Mechanism of Hologram Formation in Dich-romated Gelatin," *Applied Optics*, Vol. 9, July 1970, pp 1651--57.

[13]Dietrich Meyerhofer, "Phase Holograms in Dichromated Gelatin," *RCA Review*, Vol. 33, March 1972, p 119.

TABLE 6. PROCESSING PROCEDURE FOR DCG PROCESS

	PROCEDURE	TEMP	TIME
11.	Dichromate Gelatin Plate in 1%, 3%, or 5% solution of $(NH_4)_2Cr_2O_7$.	Rm. Temp.	5 mins.
12.	Clean glass side of plate with kem wipes.		
13.	Dry in dark in horizontal position.	Rm. Temp.	$\geqslant$2 hrs.
14.	Expose (used optical arrangements shown in Scheme 3).	Rm. Conditions	
15.	Wash in running water.	21–24° C	10 mins.
16.	Wash in distilled water.	Rm. Temp.	2 mins.
17.	Dehydrate in 50/50 solution of distilled water and Isopropanol.	Rm. Temp.	3 mins.
18.	Dehydrate in pure Isopropanol.	Rm. Temp.	4 mins.
19.	Dry in room air.	Rm. Temp.	10 mins.
20.	Oven dry.	82° C	2 hrs.
21.	Store in Desiccator over Anhydrous $CaCl_2$	Rm. Temp.	Indef.

DATA AND OBSERVATIONS ■ The diffraction efficiency data is plotted as a function of exposure, which is defined as the product of the total power in the two recording beams and the time. In taking the power readings in the first diffracted order, the plate was either rotated to produce the highest power for the brightest grating and all subsequent plane wave gratings read or, as in one case, was rotated for each grating to produce the highest possible power for each plane wave grating read.

In figure 1, the characteristic exposure curve is shown for dichromated gelatin plates sensitized in 5% ammonium dichromate solution. The recording power is high at 6.95 mW/cm^2 (milliwatts per square centimeter), and the K–ratio is 9.7. K–ratio is the ratio of intensities of the two recording beams. Because the recording power is high, the exposure time is short. Air turbulance may affect the data obtained since no canopy was used.

In figure 2, the characteristic exposure curve is shown for dichromated gelatin plates sensitized in 1 percent ammonium dichromate solution. The recording power is low

λ = 488.0nm
Spatial Freq = 1000 c/mm
k = 9.7
Recording Power = 6.95 mW/cm²
Read Out Power = 0.220 mW/cm²
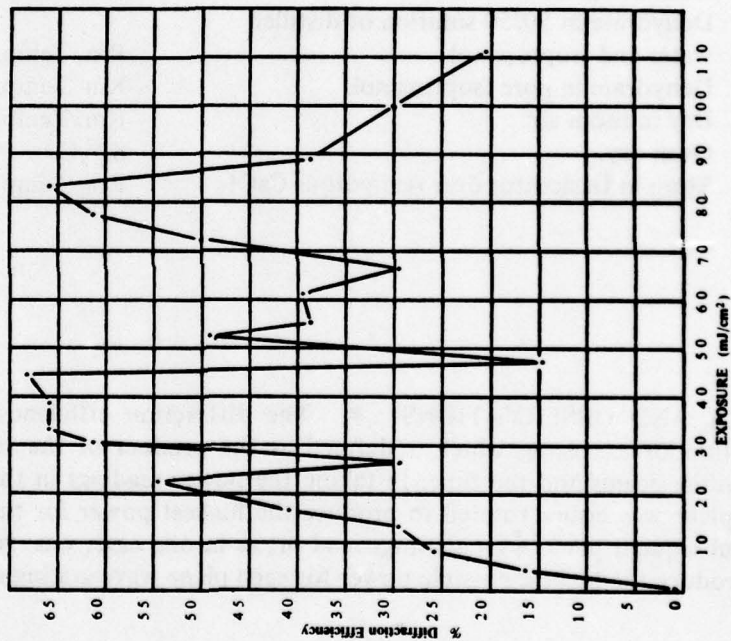Recording Temp. 21°C & %RH 55%
No Canopy

Dichromated Gelatin (5%)

% Diffraction Efficiency

EXPOSURE (mJ/cm²)

FIGURE 1. Dichromated Gelatin (5%)

λ = 488.0nm

Spatial Freq = 1580 c/mm

k = 1.03

Recording Power = 1.685 mW/cm²

Read Out Power = 0.810 mW/cm²

Recording Temp. 21°C & %RH 31%

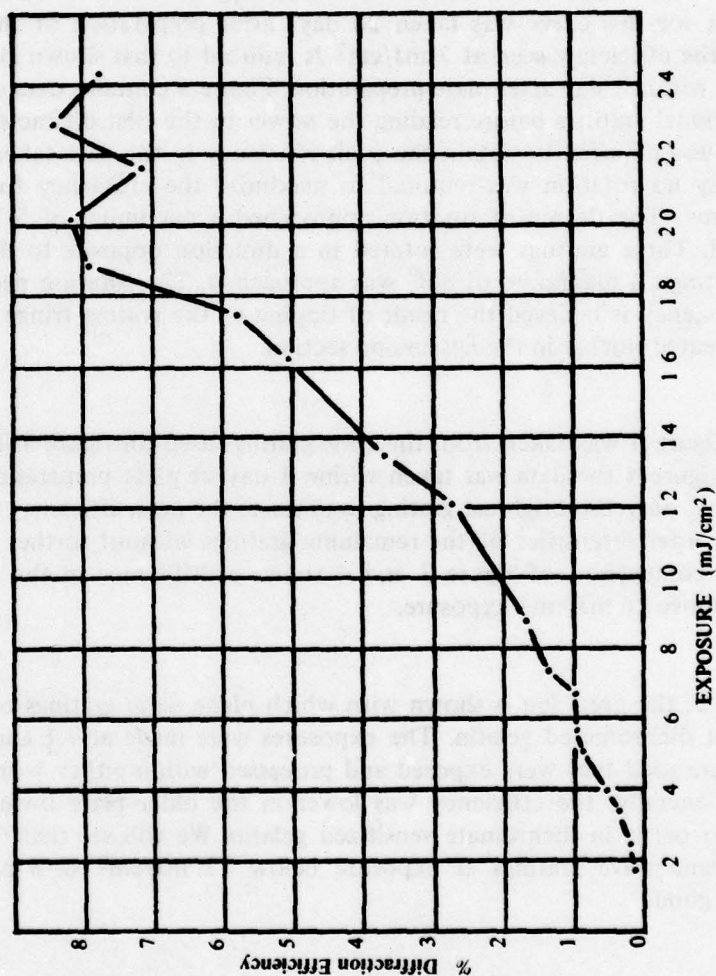% Diffraction Efficiency

EXPOSURE (mJ/cm²)

FIGURE 2. Dichromated Gelatin (1%)

at 1.685 mW/cm^2, and the K–ratio is 1.03. A canopy was used to minimize air tur-bulance. The peak efficiency appears to be in the neighborhood of 8 percent for the gelatin sensitized in the 1 percent ammonium dichromate solution.

In figure 3, the characteristic exposure curve is shown for dichromated gelatin plates sensitized in 3 percent ammonium dichromate solution. The recording power is low at 1.725 mW/cm^2 and the K–ratio is 1.02. A canopy was used to minimize air turbulance. The data for this curve was taken 20 days after preparation of the plate, and conse-quently the efficiency seen at 7 mJ/cm^2 is reduced to that shown in figure 4, which was read out within 1 day after plate preparation. Figure 3 contains data obtained by rotating the individual gratings before reading the power in the first diffracted order. Significant rotation was required to obtain the peak efficiency in the data taken above 17 mJ/cm^2. Essentially no rotation was required to maximize the efficiency for data taken below 17 mJ/cm^2. The degree of rotation approached a maximum of 5.7° for most gratings measured. Three gratings were rotated in a direction opposite to the others. For these three gratings, a maximum of 3.3° was approached. The rotation needed to produce the peak efficiency is believed the result of tipping of the grating fringe planes. This matter will be treated further in the Discussion section.

Data in figure 4 was taken from the same gratings used for figure 3. The difference being that for figure 4 the data was taken within 1 day of plate preparation and was obtained by rotating only the brightest grating to produce the peak efficiency followed by reading the first order intensities of the remaining gratings without further rotating the grating plate. A comparison of figure 3 and 4 shows a difference in the order of peaks and troughs above 26 mJ/cm^2 exposure.

In figure 5, the precision is shown with which plane wave gratings could be prepared in 3 percent dichromated gelatin. The exposures were made at 7.1 and 2.7 mJ/cm^2. Two plates were used that were exposed and processed within either 4 or 20 hours of sensiti-zation. Generally, the efficiency was lower in the older plate owing to dark reactions known to occur in dichromate sensitized gelatin. We will see that the precision of pre-paring plane wave gratings at exposure below 17 mJ/cm^2 in 3 percent dichromated gelatin is good.

28

$$\lambda = 488.0 \text{ nm}$$
$$\text{Spatial Freq} = 1580 \text{ c/mm}$$
$$k = 1.02$$
$$\text{Recording Power} = 1.725 \text{ mW/cm}^2$$
$$\text{Read Out Power} = 0.800 \text{ mW/cm}^2$$
Recording Temp 21°C & %RH 38%
Rotated
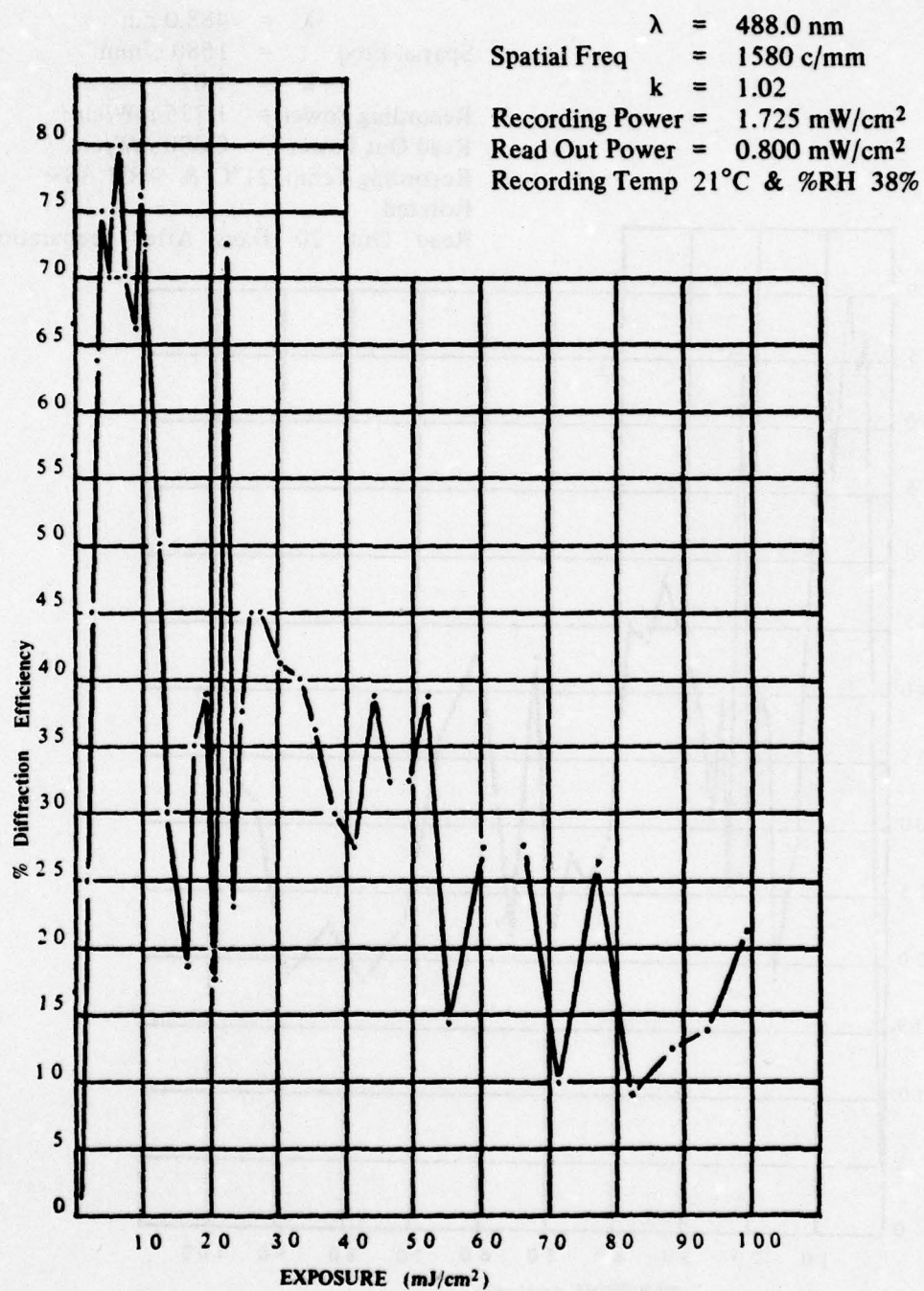Read Out 20 Days After Preparation
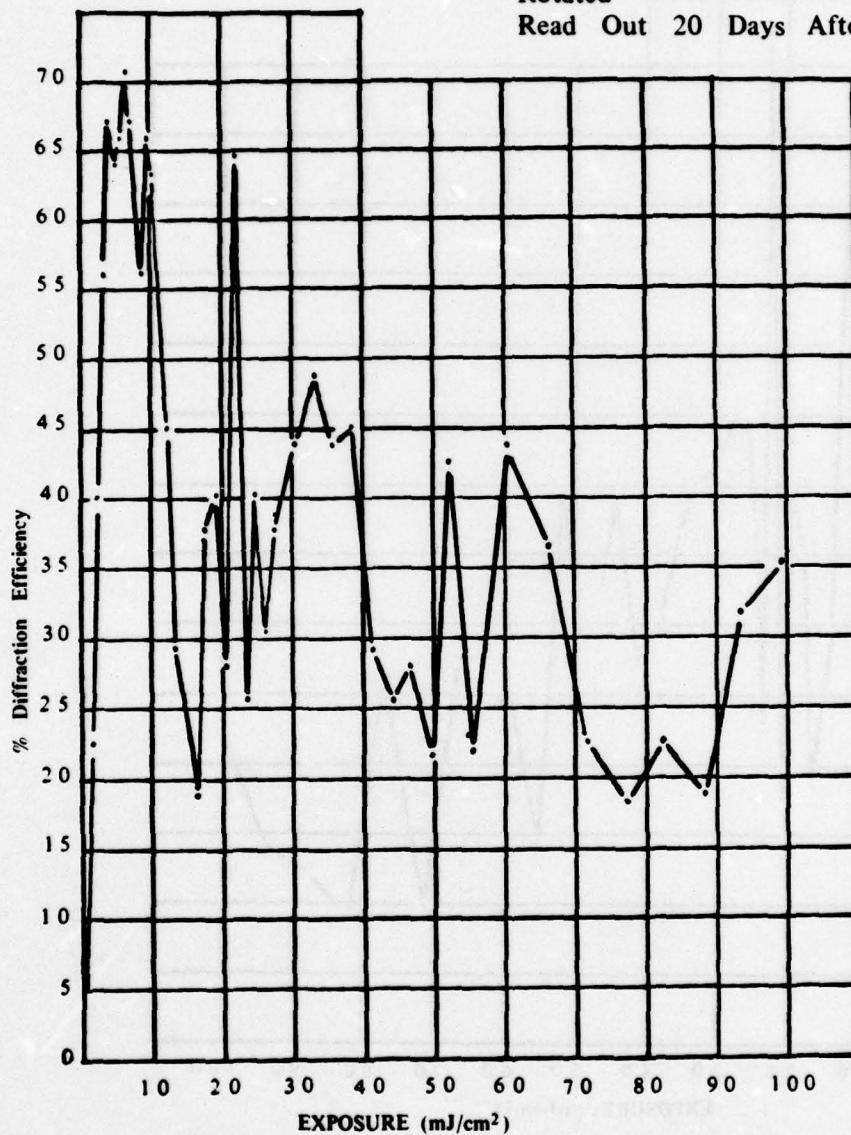
FIGURE 3.   Dichromated Gelatin (3%)
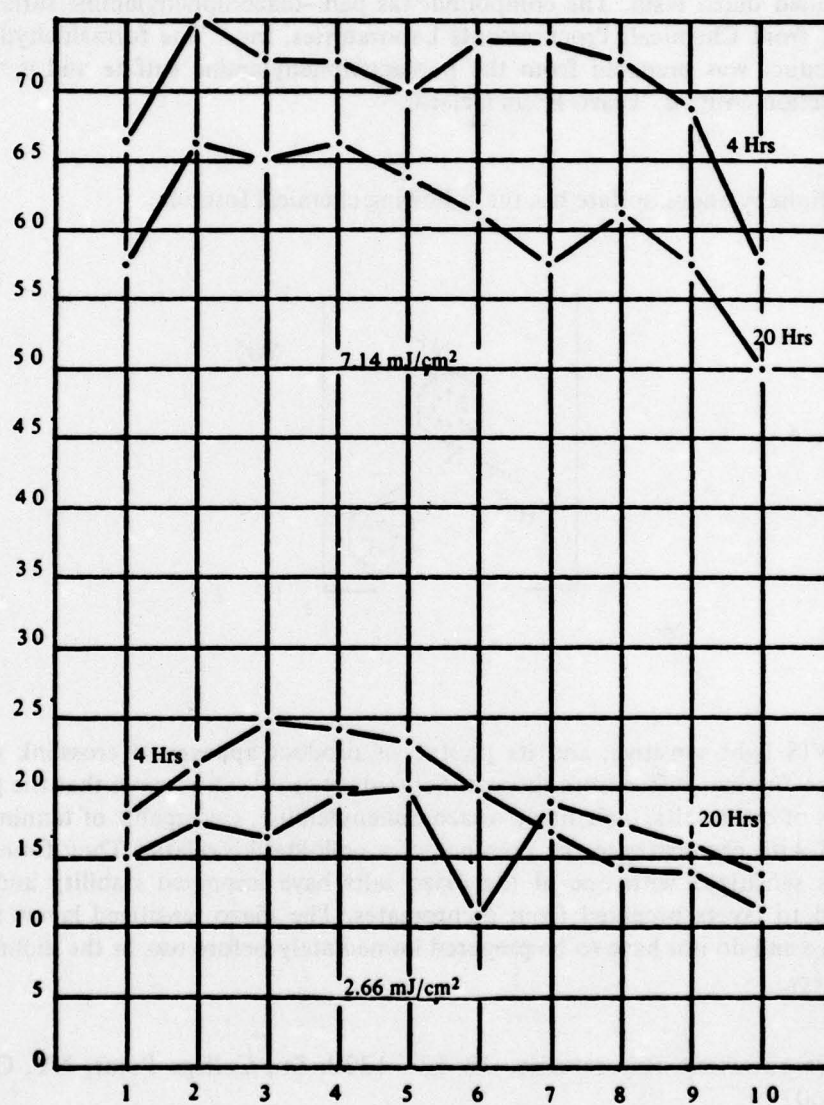
29

FIGURE 4. Dichromated Gelatin (3%)

30

FIGURE 5. Dichromated Gelatin (3%)

31

DIAZO GELATIN

BACKGROUND ■ The diazo componds are a class of aromatic organic salts having the general formula $ArN_2^+X^-$. Here X^- is one of many anions, such as Cl^-, HSO_4^-, BF_4^-, etc. Although the number of different diazo compounds is very large, this report was envolved with only one compound and its formaldehyde condensation product, which was called diazo resin. The compound was para–diazodiphenylamine sulfate and was obtained from Chemicals Procurements Laboratories, Inc.* The formaldehyde condensation product was prepared from the p–diazodiphenylamine sulfate and is treated in the next section entitled "Diazo Resin Gelatin."

The p–diazodiphenylamine sulfate has the following chemical formula:

$$\left[\begin{array}{c} N_2^+ \\ \bigcirc \\ N \\ H \quad \bigcirc \end{array} \right]_2 SO_4^=$$
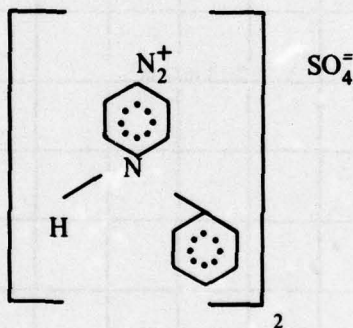
This salt is VIS light sensitive, and its photolysis product appears to crosslink gelatin directly. These findings differ from those of Schmidt et al. [14] who report that the photolysis products of diazo salts, including p–diazodiphenylamine, are capable of tanning only when reacted with chromates in the presence of a colloid–like gelatin. They found that gelatin layers sensitized with one of the diazo salts have improved stability and shelf life compared to layers prepared from dichromates. The diazo sensitized layers can be kept in storage and do not have to be prepared immediately before use, as the dichromate sensitized layers.

*Chamicals Procurement Laboratories, 18–17 130th St., College Point, NY, Catalog Number D–2602.

[14] Maximilian Paul Schmidt, Rudolf Zahn, and Wilhelm Krieger, U. S. Patent 1,762,033, *Process of Preparing Pictures to be Produced by Tanning Action*, June 3, 1930.

Still another process is described by Zemp[15] in a later patent. In this process, a hardened gelatin layer is sensitized with a diazo salt by immersing the layer in a 2 percent solution containing the diazo salt until the layer is impregnated thoroughly with the solution. After drying, the sensitized hardened gelatin layer is exposed and washed with hot water at 70° C. In the exposed areas, nitrogen gas is formed through photolysis of the diazo salt. Formation of nitrogen gas is characteristic of most diazo compounds upon exposure to actinic radiation. The hot water bath expands the nitrogen gas in the hardened gelatin, and the gas slowly escapes through the swollen and soft gelatin. Zemp found that the gelatin could be washed off in the exposed parts upon gently rubbing the layer with a cotton pad. A relief image remains in the unexposed areas of the layer. This process is minimized in this study by the manner of preparation of plane wave gratings in diazo salt sensitized, hardened gelatin. The method of preparation will be described next.

SENSITIZATION AND PROCESSING PROCEDURES ▪ The procedure set forth in table 6 was used to sensitize and process the diazo gelatin plates. Step 11 is changed to read, Diazotize Gelatin Plate in 1 percent solution of p-diazodiphenylamine sulfate. The sensitization follows the gelatin plate preparation shown in table 5. However, the procedure of table 5 was modified to oxidize the gelatin layer prior to the sensitization of several plates. The data taken from these plates will be indicated as obtained with oxidized gelatin.

This procedure for oxidizing the gelatin layer is shown in table 7. After treatment of the plate in $Br_2 - H_2O$ (50 milliliters of Sol. B with 5 ml Sol. A) in a fume hood, an additional 5 ml of Sol. A is added if plate is still colored. Perfectly clear plates should be obtained. Data was taken using 488.0 nm radiation and the canopy to minimize air currents.

---

[15]Rene Robert Zemp, *Process for Producing Images*, U. S. Patent 2, 729,562, January 3, 1956.

TABLE 7. OXIDIZED GELATIN PLATE PREPARATION

	PROCEDURE	TEMP	TIME
1.	Fix in Kodak Fixer F-24.	Rm. Temp.	10 mins.
2.	Wash in running water.	21–24° C	15 mins.
3.	Oxidize in Br_2-H_2O.ª	Rm. Temp.	≥15 mins.
4.	Wash in running water.	21-24° C	15 mins.
5.	Rinse in distilled water with 5 drops of photo-flow 200 per liter H_2O.	Rm. Temp.	30 secs.
6.	Dry completely in room air.	Rm. Temp.	2 hrs.

a. The Bromine-Water (Br_2-H_2O) was prepared as follows:

Solution A – 5 grs. $KMnO_4$/liter of distilled water.
Solution B – 50 grs KBr in 500 ml. distilled water. Add 10 ml. conc. H_2SO_4
and dilute to make 1 liter with distilled water. One part solution A is added to
ten parts solution B.

DATA AND OBSERVATIONS ■   The efficiency data is plotted as a function of exposure. As before, either the plate was rotated to produce the maximum power reading for the brightest grating and all subsequent plane wave gratings read or it was rotated for each grating to produce the highest possible power from each grating.

In figure 6, the characteristic exposure curves are shown for diazo gelatin plates at two different K–ratios. The efficiency is seen to drop at the higher K–ratios. Note that the efficiency does not rise significantly until after an exposure of 120 mJ/cm^2 at K = 1.08.

In figure 7, the characteristic exposure curves are shown for diazo gelatin at higher exposures than for figure 6. Three different K–ratios are displayed. A series of four peaks are seen at K = 1.02 and 9.20. Generally, the efficiency decreases as K–ratios increase.

In figure 8, the characteristic exposure curve is shown for diazo gelatin for which care was taken to insure minimal motion between the recording material and the recording light interference pattern. This was done by waiting between stage travels of the recording platen and when the exposure was actually initiated so as to minimize mechanical motion in the plate holder stages. A series of five peaks are displayed that correspond with the series of peaks described in the characteristic exposure curves for figures 6 and 7.

λ = 488.0 nm
Spatial Freq = 1580 c/mm
k = 1.08 & 48.5
Recording Power = 10.8 &
9.90 mW/cm²
Read Out Power = 0.800 mW/cm²
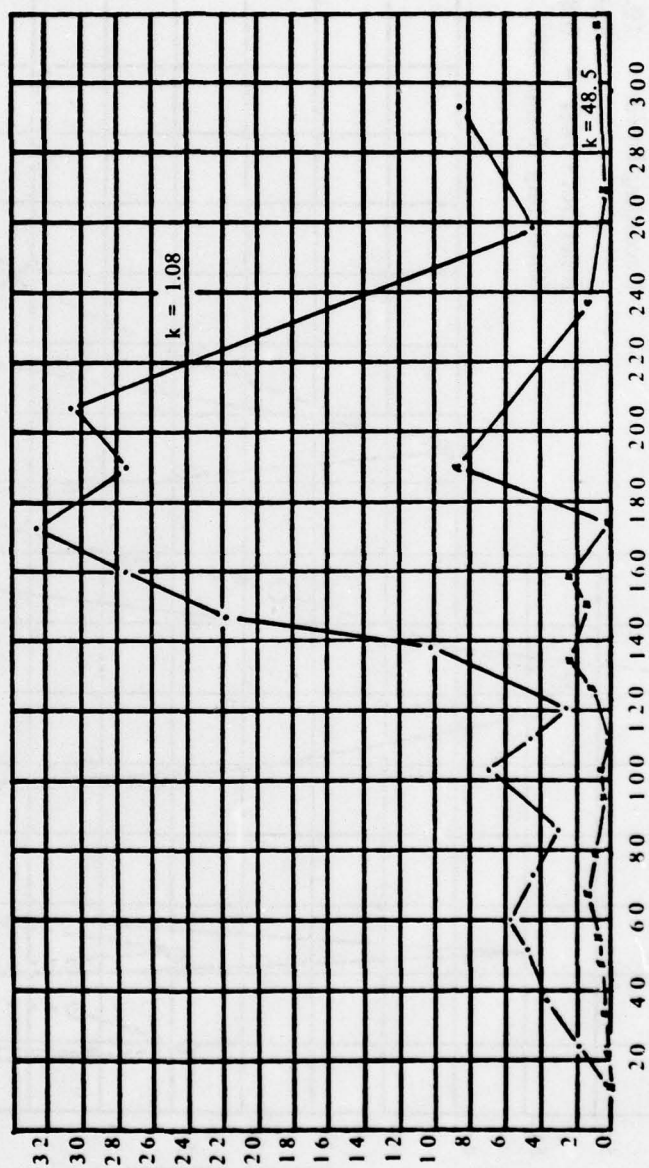Recording Temp 20°C & %RH 52%

k = 1.08

k = 48.5

FIGURE 6.   Diazo Gelatin

35

Spatial Freq = 1580 c/mm

λ = 488.0nm
k = 1.02 & 9.20 & 48.5

Recording Power = 10.3 & 10.2 & 9.90 mW/cm^2
Read Out Power = 0.800 mW/cm^2
Recording Temp. 20°C & %RH 55%

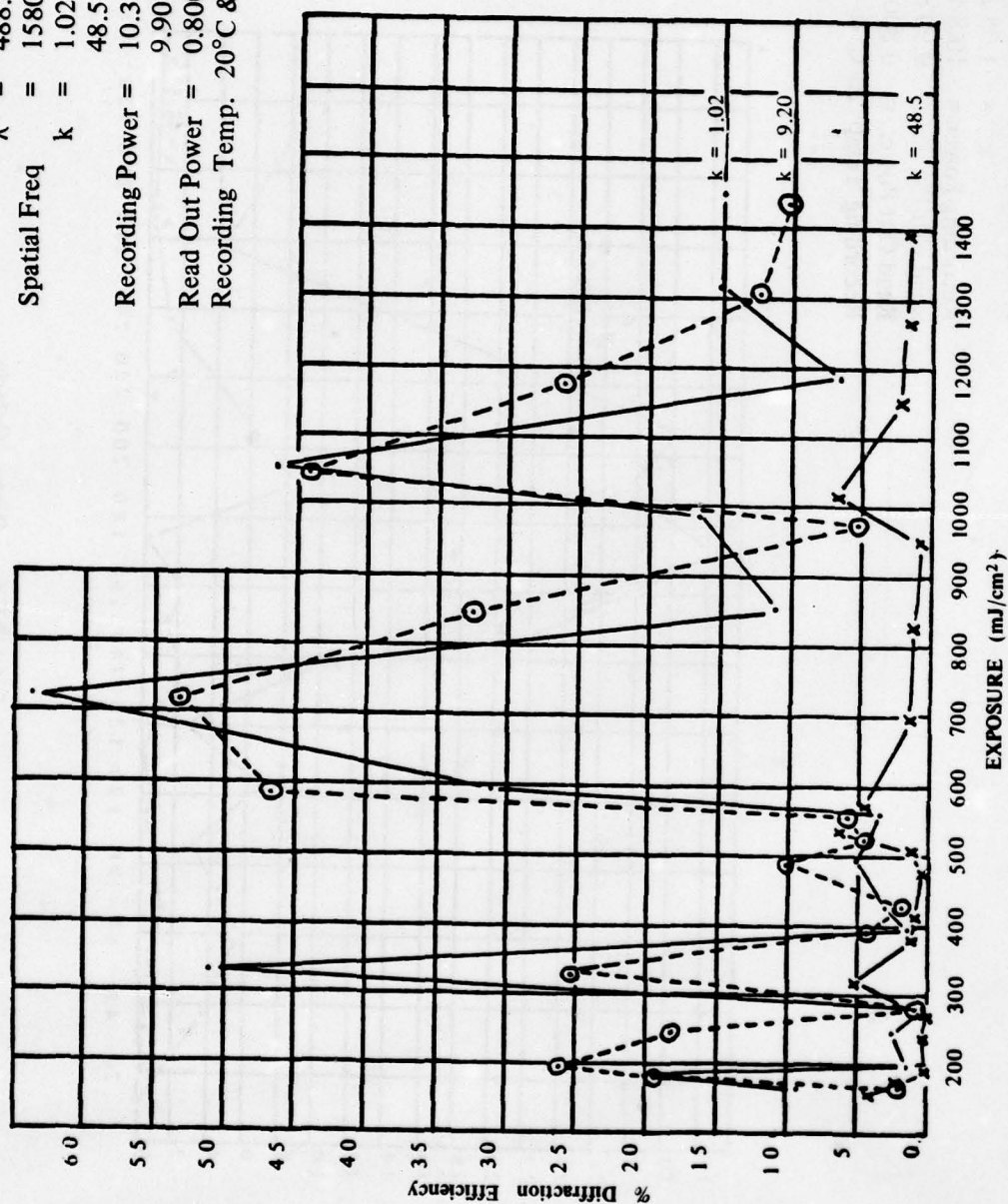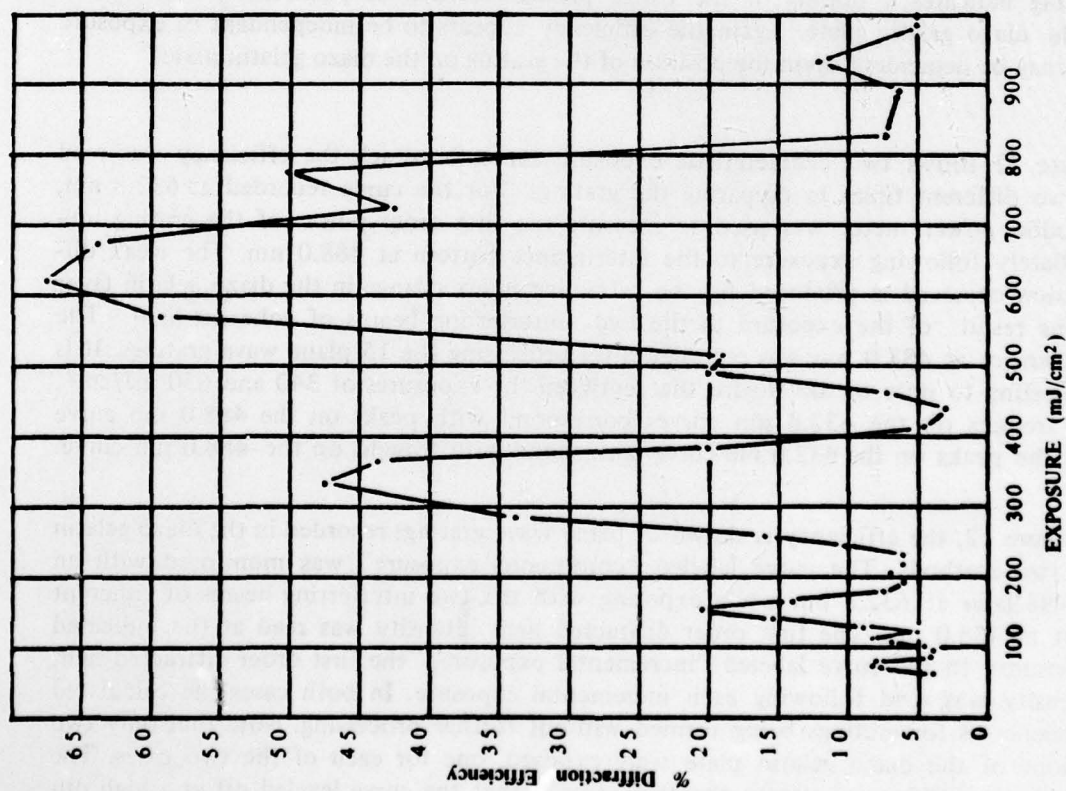k = 1.02

k = 9.20

k = 48.5

EXPOSURE (mJ/cm^2)

% Diffraction Efficiency

60
55
50
45
40
35
30
25
20
15
10
5
0

200 300 400 500 600 700 800 900 1000 1100 1200 1300 1400

FIGURE 7. Diazo Gelatin

Spatial Freq
Recording Power =
Read Out Power =
Recording Temp 20°C & %RH 38%

λ = 488.0nm
= 1580 c/mm
k = 1.05
8.10 mW/cm²
0.800 mW/cm²

% Diffraction Efficiency

EXPOSURE (mJ/cm²)

FIGURE 8. Diazo Gelatin

37

In figure 9, the statistics are shown of exposing the diazo gelatin plates with 7 to 10 identical exposures. The exposures chosen correspond to either a peak or trough on the characteristic exposure curve shown in figure 8. Two diazo gelatin plates were used for the series of 37 exposures. The results displayed in figure 9 show no obvious dependence of efficiency on exposure, and the efficiency appears dependent upon the position of the grating on the plate.

In figure 10, the statistics are shown for exposing an oxidized, diazo gelatin plate with 10 identical exposures. The exposure chosen corresponds with a peak on the characteristic exposure curve for figure 8. The data was taken in the two modes described earlier. The first mode was taken in which the plane wave grating was rotated at position 4 until a peak diffraction efficiency was observed and each grating was subsequently read. The efficiency for these readings are shown as the stippled lines except where the readings were identical to those taken by the second mode. The second mode was taken by rotating each plane wave grating on the diazo gelatin plate to produce a peak power reading that was then read. The difference in the efficiency seen for the two modes of reading indicates a tipping of the fringe planes recorded at positions 1–3 and 7–10 in the diazo gelatin plate. Again the efficiency appears to be independent of exposure and may be dependent upon the position of the grating on the diazo gelatin plate.

Figure 11 shows two characteristic exposure curves in which the efficiency was read at two different times in preparing the gratings. For the curve recorded at 632.8 nm, a Jodon power meter was used to measure the first order power of the grating immediately following exposure to the interference pattern at 488.0 nm. The weak diffraction observed is produced by the refractive index change in the diazo gelatin layer as the result of the exposure to the two interferring beams of coherent light. The efficiencies at 488.0 nm was recorded after processing the 15 plane wave gratings. It is interesting to note on the figure that between the exposures of 340 and 630 mJ/cm^2, the troughs on the 632.8 nm curves correspond with peaks on the 488.0 nm curve and the peaks on the 632.8 nm curve correspond with troughs on the 488.0 nm curve.

In figure 12, the efficiency is shown of plane wave gratings recorded in the diazo gelatin by two methods. The curve labeled "continuous exposure" was monitored with an He–Ne laser at 632.8 nm while exposing with the two interferring beams of coherent light at 488.0 nm. The first order diffracted light intensity was read at the indicated exposures. In the curve labeled "incremental exposure," the first order diffracted light intensity was read following each incremental exposure. In both cases the calculated efficiency is for gratings being formed without further processing. Note that only two regions of the diazo gelatin plate were exposed, one for each of the two cases. The significant difference between the two cases is that the curve leveled off at a high diffraction efficiency, about 1.5 percent in the case for the continuous exposure, and that the curve peaked at only 0.36 percent before returning to near zero efficiency in the case for the incremental exposure.

38

λ = 488.0 nm

Spatial Freq = 1580 c/mm
k = 1.07
Recording Power = 9.40 mW/cm²
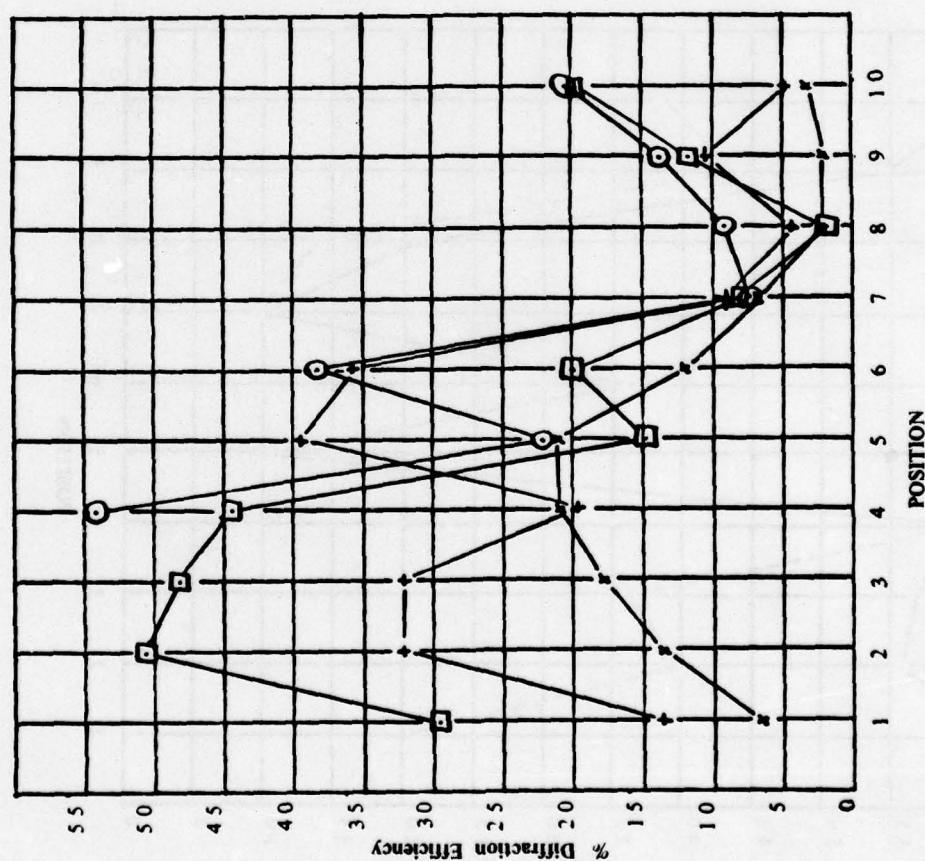Read Out Power = 0.810 mW/cm²
Recording Temp. 22°C & %RH 34%
EXPOSURE
(mJ/cm²)
660. ⊙
450. ▣
360. +
210. x

FIGURE 9. Diazo Gelatin – Statistics

FIGURE 10. Oxidized Diazo Gelatin – Statistics

λ = 488.0nm
Spatial Freq = 1580 c/mm
k = 1.06
Recording Power = 9.25 mW/cm²
Read Out Power = 0.825 mW/cm²
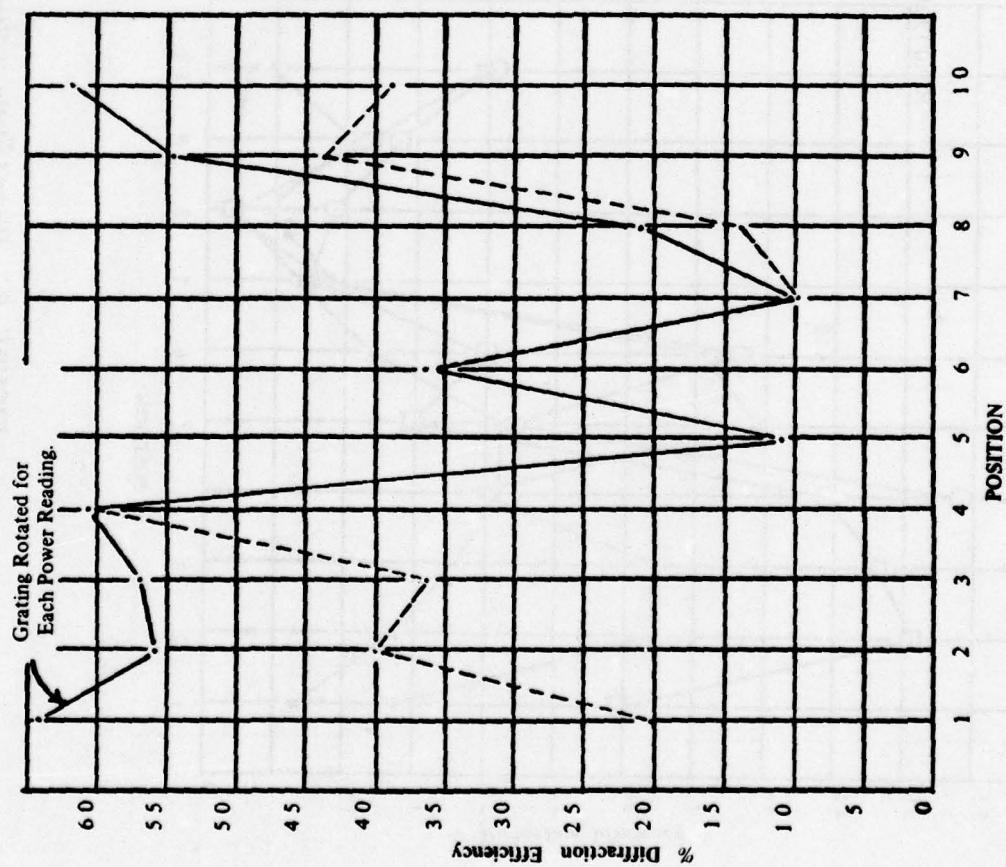Recording Temp 21°C & %RH 46%
EXPOSURE = 650 mJ/cm²

Grating Rotated for
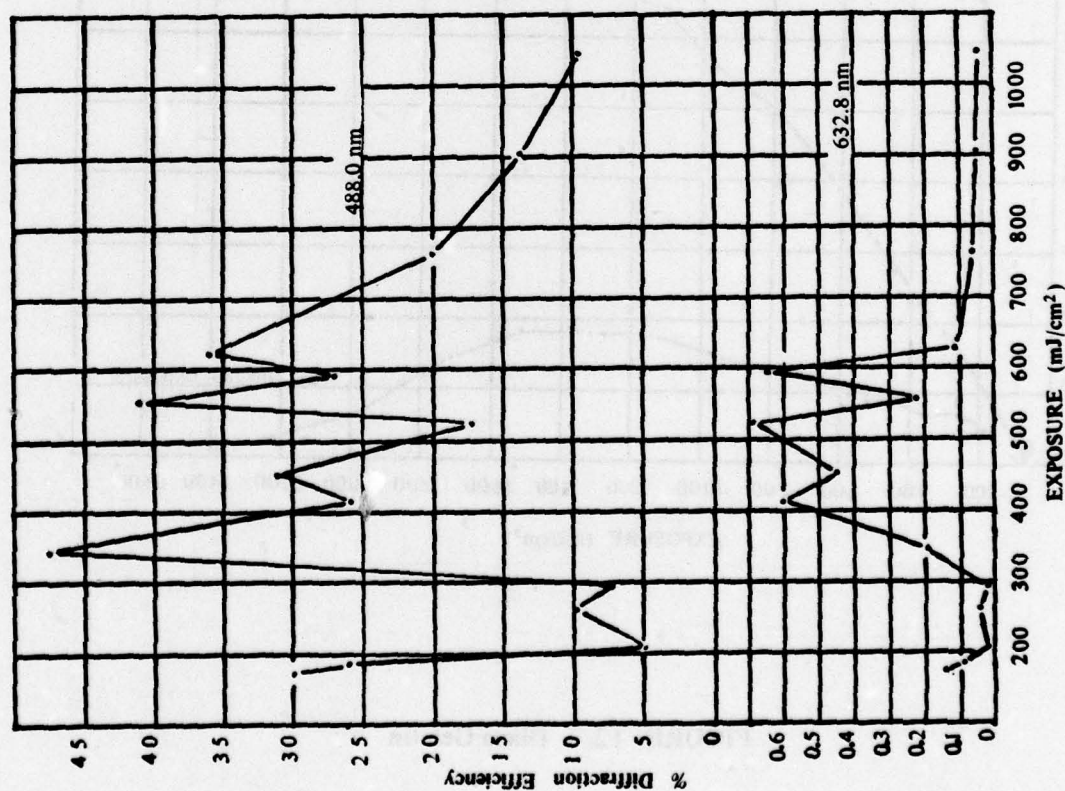Each Power Reading.

% Diffraction Efficiency

POSITION

Spatial Freq λ = 488.0 nm

Spatial Freq = 1580 c/mm

k = 1.18

Recording Power = 10.9 mW/cm²

Read Out Power @ 488.0 nm = 0.610 mW/cm²

Read Out Power @ 632.8 nm = 11.0 mW

Recording Temp 23°C & %RH 46%

FIGURE 11. Diazo Gelatin

41

$$\lambda \quad = \quad 488.0 \text{ nm}$$

Spatial Freq $\quad = \quad$ 1580 c/mm

$$k \quad = \quad 1.18$$

Recording Power $=$ 10.9 mW/cm^2

Read Out Power

@ 632.8 nm $\quad = \quad$ 11.0 mW

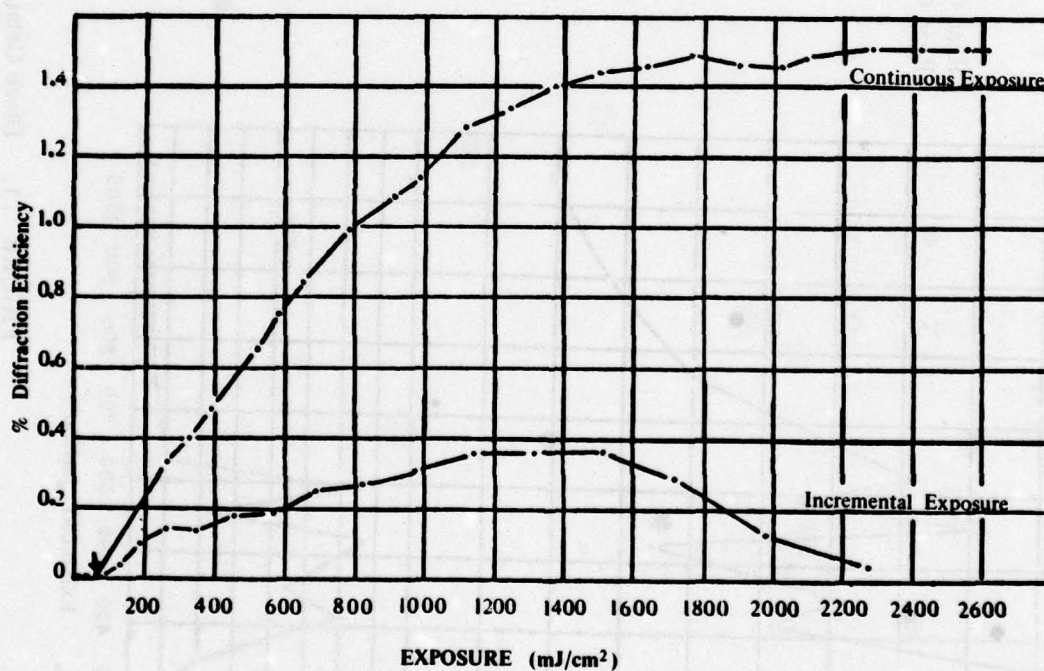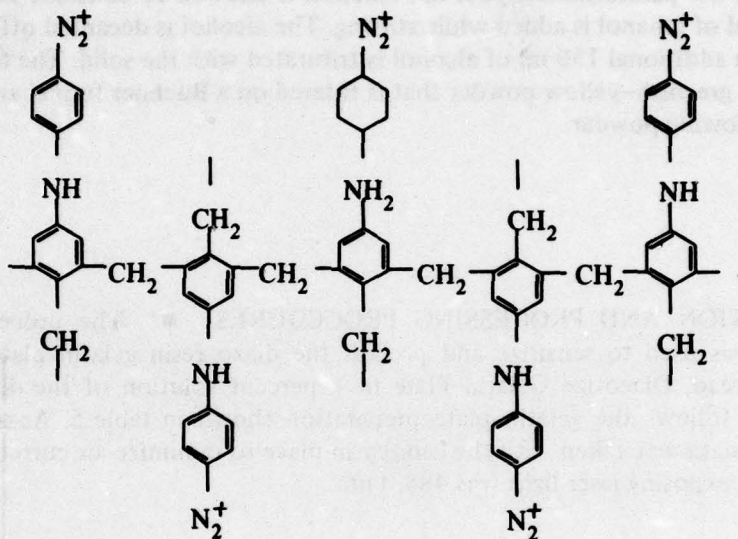Recording Temp 23°C & %RH 46%

FIGURE 12. Diazo Gelatin

42

DIAZO RESIN GELATIN

BACKGROUND ▪ The diazo resin used to sensitize the gelatin is a formaldehyde condensation product of para–diazodiphenylamine sulfate. Hepher[16] has suggested the following structure:

$$N_2^+ \qquad N_2^+ \qquad N_2^+$$

As late as 1965, Reichel stated that p–diazodiphenylamine has practically no tanning effect on colloidal proteins.[17] Such colloids were believed to be tanned only when the photolysis products of the diazo salt were reacted with chromates. However, in 1937, Zahn found that the higher molecular weight diazos, such as the diazo resin, would readily tan colloidal proteins without treating the sensitized and exposed layer with a chromate solution.[18]

---

[16]M. Hepher, "The Photo--Resist Story--from Niepce to the Modern Polymer Chemist" *The Journal of Photographic Science*, Vol. 12, 1964, p 184.

[17]Maximilian Karl Reichel, U. S. Patent 3,189,451, *Light Sensitive Reproduction Material Comprising a Colloid Containing An Aldehyde and a Diazotized Phenylamine Compound*, June 15, 1965.

[18].Rudolf Zahn, U. S. Patent 2,100,063, *Process For The Production of Tanned Pictures*, November 23, 1937.

The procedure for preparing the formaldehyde condensate of p—diazodiphenylamine sulfate is given in a U. S. patent by Seven and Miyashiro.[19] Approximately 20 ml of concentrated sulfuric acid is placed in a round—bottom flask equipped with a suitable stirrer and brought to 0° C with an ice—salt bath. After 11.2 grams of p—diazodiphenylamine sulfate is added, the mixture is brought to 6° C. A total of 1.5 grams of paraformaldehyde, powder is added at such a rate that the temperature does not exceed 10° C. After adding the paraformaldehyde, the reaction is allowed to continue for 30 minutes. Then, 150 ml of ethanol is added while stirring. The alcohol is decanted off the taffy—like solid, and an additional 150 ml of alcohol is triturated with the solid. The taffy—like solid changes to a greenish—yellow powder that is filtered on a Buchner funnel and air—dried to give a free—flowing powder.

SENSITIZATION AND PROCESSING PROCEDURES ▪ The procedure outlined in table 6 was used to sensitize and process the diazo resin gelatin plates. Step 11 is changed to read, Diazotize Gelatin Plate in 1 percent solution of the diazo resin. The sensitization follows the gelatin plate preparation shown in table 5. As with the Diazo Gelatin, the data was taken with the canopy in place to minimize air currents. The wavelength of the exposing laser light was 488.0 nm.

DATA AND OBSERVATIONS ▪ The efficiency data is plotted as a function of exposure. Upon taking the power readings in the first diffracted order, the plate was rotated to produce the highest possible power for the brightest grating, and all subsequent plane wave gratings were read without further rotation. However, one series of plane wave gratings was read out in which the plate was rotated for each grating to detect tipping of the grating fringe planes. No tipping of the fringe planes was observed.

In figure 13, the characteristic exposure curve is shown for diazo resin gelatin in which the canopy was used, but no special precautions were taken to minimize plate motion. Although the shape of the characteristic exposure curve is seen to be the same as that for the diazo gelatin (see figures 7 and 8), the peak efficiency is seen to be only 15 percent, which is below the 67.5 percent observed for the diazo gelatin.

---

[19]Raymond P. Seven and James J. Miyashiro, U. S. Patent 2,679,498, *Preparation of Diazo Condensation Polymers*, May 25, 1954.
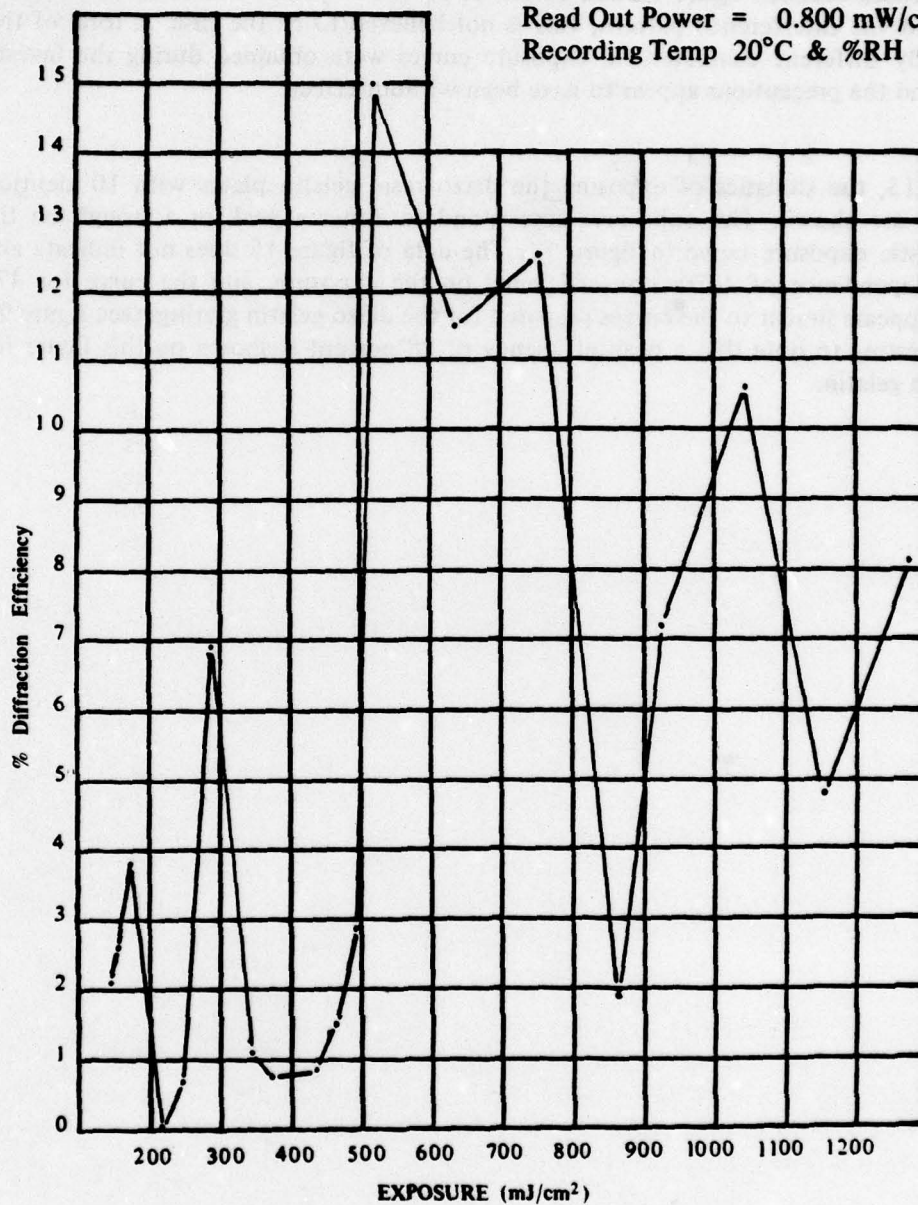
44

FIGURE 13. Diazo Resin Gelatin

In figure 14, the characteristic exposure curve is shown for diazo resin gelatin in which the canopy was used to minimize air currents, and the precaution was taken to insure minimal motion between the plane wave grating and the interference pattern. Although the differences between figure 13 and 14 might be due to possible motions between the grating and the interference pattern, this is not believed to be the case. A total of five significantly different characteristic exposure curves were obtained during the investigations, and the precautions appear to have been without effect.

In figure 15, the statistics of exposing the diazo resin gelatin plates with 10 identical exposures are shown. The exposures correspond to either a peak or a trough on the characteristic exposure curve in figure 14. The data of figure 15 does not indicate any obvious dependence of diffraction efficiency on the exposure, and the curve for 475 mJ/cm^2 appears similar to the curves prepared for the diazo gelatin gratings (see figure 9). It is interesting to note that a peak efficiency of 28 percent is shown on this figure for diazo resin gelatin.

46

λ = 488.0 nm
Spatial Freq = 1580 c/mm
k = 1.09
Recording Power = 9.0 mW/cm^2
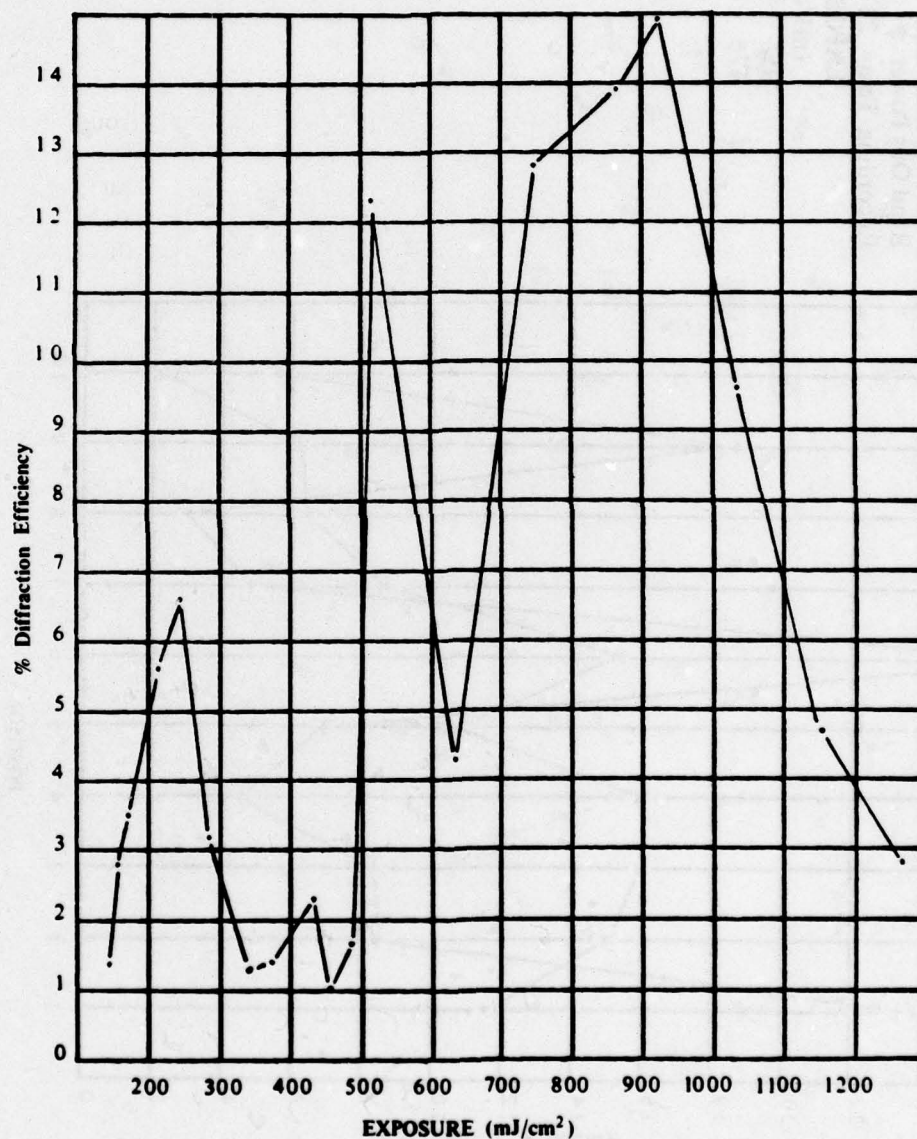Read Out Power = 0.790 mW/cm^2
Recording Temp 22°C & %RH 46%

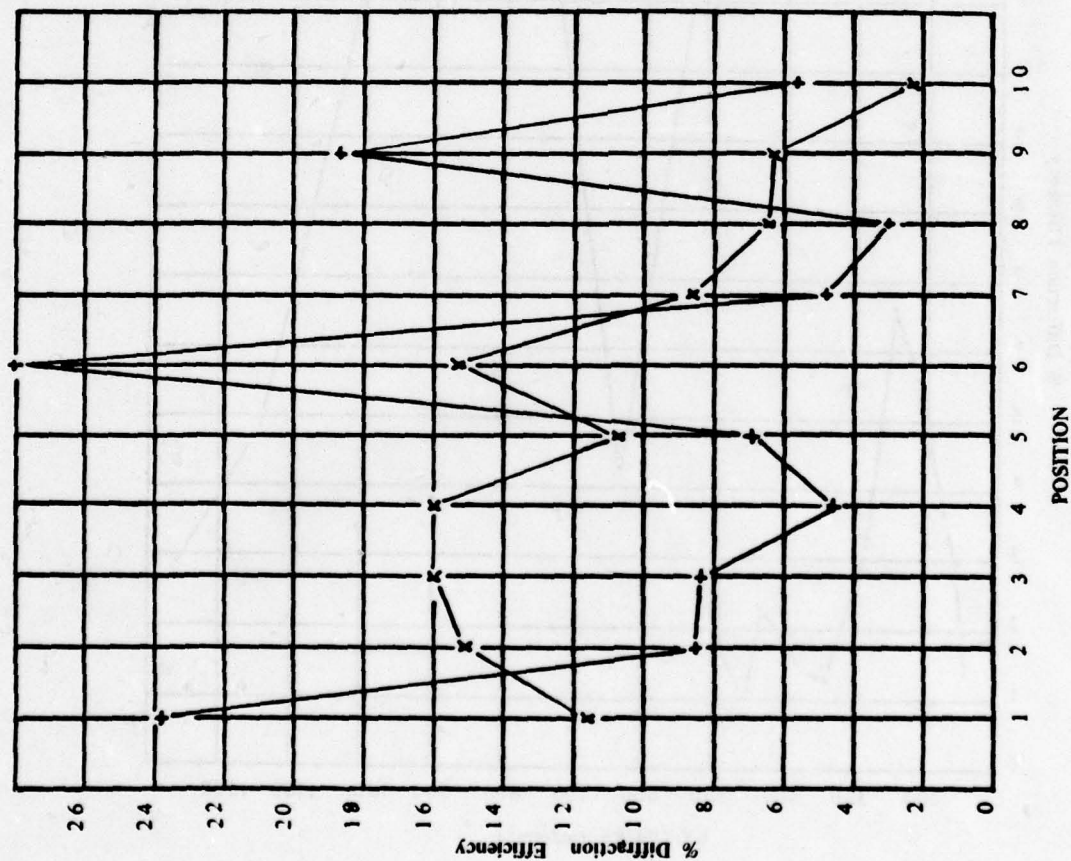FIGURE 14.   Diazo Resin Gelatin

47

FIGURE 15. Diazo Resin Gelatin

SILVER HALIDE (SENSITIZED) GELATIN

BACKGROUND ■ Photographic relief images in gelatin are formed when the oxidation products of certain developers promote tanning of the emulsion. Tanning bleaches have also been used to produce relief images. Altman[20] and Smith[21] described relief images at low spatial frequencies (e.g. below 200 c/mm), which they attributed to tanning effects. However, their treatment does not suggest the possibility of producing images at high spatial frequencies whose structure consists of variations in the refractive index of the gelatin.

The possibility of producing index–of–refraction differences in gelatin with either tanning developers or tanning bleaches was suggested by our study of the work of Lamberts and Kurtz involving a reversal bleaching process that produces low flare light in holograms.[22] In their process, a special tanning developer of the pyrocatechol type is used that promotes tanning of the gelatin in regions where metallic silver is developed. Tanning is also promoted by the bleach used.

The reversal bleaching process consists of developing in Kodak special developer SD–48, bleaching without fixing in Kodak R–9 bleach, clearing in each of Solutions A & B of Kodak stain remover S–13, and drying. The Sodium sulfite in the developer is in a small amount to reduce atmospheric oxidation of the developer without counteracting the tanning action of the pyrocatechol. Sodium sulfate in the developer prevents excessive swelling of the gelatin during development. The R–9 bleach that is used also exerts tanning effects and acts to oxidize metallic silver to a soluble salt, which is removed, leaving the unfixed silver halide intact. The reversal bleaching process has been shown to reduce the amount of scattering and flare attributed to the surface irregularities in the gelatin.

---

[20] J. H. Altman, "Pure Relief Images on Type 649--F Plates," *Applied Optics*, Vol. 5, No. 10, October 1966, p 1689.

[21] Howard M. Smith, "Photographic Relief Images," *J. Optical Society of American*, Vol. 58, No. 4, April 1968, p 533.

[22] R. L. Lamberts and C. N. Kurtz, "Reversal Bleaching for Low Flare Light in Holograms," *Applied Optics*, Vol. 10, No. 6, June 1971, p 1342.

Using the properties of the reversal bleach method, we sought to prepare plane wave gratings free of silver metal and silver halide. The grating structures would be formed solely as variations in refractive index in gelatin. The reversal bleaching process consisting of developing, bleaching, and clearing, followed by fixing, dehydrating in isopropanol, and drying would produce the pure gelatin gratings. Our own experiments with a comparative nontanning developer, Kodak D–19, and with a concentrated nitric acid bleach, believed to be nontanning, indicate that Kodak D–19 developer produces the best results when used with the Kodak R–9 bleach. Tanning is believed to be caused by Cr^{+3} reduction product of the R–9 bleach. Considering the large amount of sodium sulfite in the developer, we believe that D–19 exerts a minimum of tanning. Fixing in a nonhardening fixer, such as Kodak F–24, would then result in a grating recorded in pure gelatin whose structure consists of refractive index variations in the gelatin.

PROCESSING PROCEDURE ■ The essential steps to the SHG process are shown in figure 16 and described in table 8. Kodak 649F plates were exposed in the optical arrangement shown earlier in Schemes 2 and 3. Scheme 2 was used in the preliminary work to verify the process. This work involved studies with Kodak special developer, SD 48, Kodak developer, D–19, Kodak reversal bleach, R–9, and a concentrated nitric acid bleach. Although this work will not be described in further detail, it did show that Kodak developer, D–19, and Kodak reversal bleach, R–9, to be the best combination of developer and bleach for demonstrating the SHG process. Scheme 3 was used for the bulk of the work reported here for the SHG process. The 514.5 nm line from the argon ion laser was used to make the grating exposures. The exposure parameters were exposure time, ratio of the two overlapping beam intensities (K–ratio), and spatial frequencies. The SHG process involves developing, bleaching, clearing, fixing, dehydrating in isopropanol, and drying. The exposed gratings were developed in the Kodak D–19 without fixing. The gratings were then bleached in Kodak R–9 bleach, which removed the silver metal as shown in figure 16.
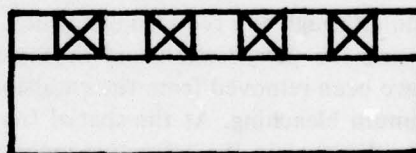
50

EXPOSE
&
DEVELOP
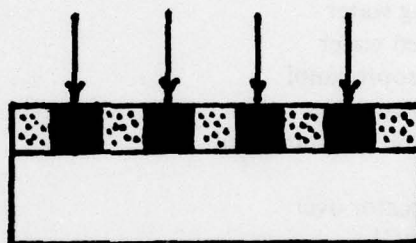
BLEACH
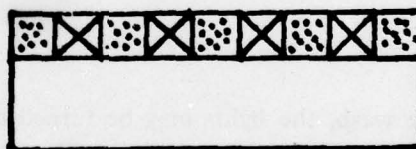
FIX
&
DRY

FIGURE 16. Diagram of the Emulsion Cross Section
for the SHG Process

51

TABLE 8.   PROCESSING PROCEDURE FOR SHG PROCESS

	STEP	TIME	TEMP °C
1.	Develop, Kodak D–19	5 min.	20
2.	Stop Bath, Kodak SB-1	15 sec.	18-21
3.	Rinse, running water	1 min.	18-21
4.	Bleach, Kodak R–9	3 min.	18-21
5.	Wash, running water	10 min.	18-21
6.	Clear, Kodak S-13, Solution B	1 min.	18-21
7.	Wash, running water	5 min.	18-21
8.	Fix, Kodak F–24	3 min.	18-21
9.	Wash, running water	10 min.	18-21
10.	Rinse, distilled water	2 min.	18-21
11.	Rinse, 50% Isopropanol 50% distilled water	3 min.	18-21
12.	Dehydrate, 100% Isopropanol	4 min.	18-21
13.	Dry, in air	30 min.	18-21
14.	Dry, in Desiccator over Anhyd. CaCl$_2$	15 hrs.	18-21

After a 10–minute wash, the lights may be turned on, and one can observe diffraction in the grating regions owing to the remaining silver halide and observe clear, but tanned, gelatin. The Kodak S–13, Solution B clearing bath will remove any remaining potassium dichromate not removed in the wash bath. The observed diffraction persists following the fixing and wash, although at a reduced efficiency. However, the diffraction efficiency will increase following the dehydration and drying steps. At this point, all silver metal and silver halide have been removed from the emulsion, and the maximum tanning occurs in regions of maximum bleaching. At the spatial frequencies considered, the diffraction is attributed to a modulation in the refractive index within the gelatin emulsion. Table 9 gives formulas for the Kodak processing solutions used. The Kodak developer, D–19, is a high contrast developer known to exert very little tanning effect because of the large quantity of sodium sulfite present. The primary tanning agent is believed to be Cr^{+3}. The nonhardening fix is used so that no further hardening of the gelatin would occur that in turn would reduce the diffraction efficiency of the plane wave gratings.

TABLE 9. KODAK PROCESSING SOLUTIONS

KODAK D-19 DEVELOPER

Distilled Water [50°C]	1.0 liter
ELON [p-Methylaminophenol Sulfate]	4.4 grs
Sodium Sulfite, desiccated	192.0 grs
Hydroquinone	17.6 grs
Sodium Carbonate, desiccated	96.0 grs
Potassium Bromide	10.0 grs
Distilled Cold Water to Make	2.0 liters

KODAK SB-1 STOP BATH

Distilled Water	4.0 liter
Acetic Acid [28%]	48.0 ml
[28% Acetic Acid is prepared by mixing 3 parts glacial acetic acid with 8 parts distilled water]	

KODAK R-9 BLEACH BATH

Distilled Water	1.0 liter
Potassium Dichromate	9.5 grs
Sulfuric Acid, conc.	12.0 ml

KODAK S-13 STAIN REMOVER, SOLUTION B

Distilled Water	750.0 ml
Sodium Bisulfite	10.0 grs
Distilled Water to Make	1.0 liter

KODAK F-24 NON-HARDENING FIX

Distilled Water [50°C]	500.0 ml
Sodium Thiosulfate [Hypo]	240.0 grs
Sodium Sulfite, desiccated	10.0 grs
Sodium Bisulfite	25.0 grs
Distilled Cold Water to Make	1.0 liter

53

MODIFIED PROCEDURE ▪ To study the effects of pH on the tanning process of the Kodak R–9 bleach, the processing procedure was modified to study three different types of solutions. In the first modified procedure, the running water wash was replaced with three containers of dilute sulfuric acid of known pH. The first container had 400 ml of the dilute acid, and the SHG plate was washed in it for 4 minutes at 18 to 21° C. The second and third containers had 300 ml of the dilute acid. The plate was washed in each container for 3 minutes at 18 to 21°C. Subsequently, each plate was processed in the dilute acid wash for a total of 10 minutes for steps 5 and 9 of the processing procedure shown in table 8. Note that steps 6 and 7 of the processing procedure were eliminated for the purpose of this study. Three dilute sulfuric acid wash baths at pH near 1.7, 3.9, and 4.7 were used to process three different SHG plates. Tap water was used to produce the wash baths at pH of 7.4.

In the second modified procedure, steps 5 and 6 of the processing procedure shown in table 8 were replaced with an acid rinse of known pH. Here four different sulfuric acid rinse waters were prepared at pHs of 0.8, 3.6, 4.5, and 5.9. Also, tap water was used to produce a rinse bath at a pH of 7.5. The SHG plates were processed in the respective acid rinse waters for 3 minutes at a temperature in the 18 to 21° C range before placing them in a running water wash, step 7.

The third modified procedure was to replace steps 5 and 6 of the processing procedure (Table 8) with a buffer rinse of known pH. Here, three different acetic acid, sodium acetate buffer solutions were prepared for pHs of 3.9, 4.6, and 5.1. The SHG plates were processed in the respective buffer rinse waters for 3 minutes at 18 to 21° C before placing them in a running water wash, step 7.

DATA AND OBSERVATIONS ▪ The plane wave gratings initially prepared using both the tanning developer, Kodak special developer SD–48, and the tanning bleach, Kodak R–9 reversal bleach, had a peak diffraction efficiency near 2.5 percent for an exposure of 175 μJ/cm^2, at a wave length of 632.8 nm, and a spatial frequency of 1,000 c/mm. The angular band width at full width, half maximum (FWHM) was approximately 3 degrees. The plane wave gratings prepared using the concentrated nitric acid bleach with either the Kodak special developer SD–48 or the Kodak developer D–19 had peak diffraction efficiencies of 1.1 percent and 1.9 percent, respectively. These also were prepared at a wavelength of 632.8 nm and a spatial frequency of 1,000 c/mm.

54

In figure 17, the characteristic exposure curve is shown for plane wave gratings prepared using the nontanning developer, Kodak D-19, and the tanning bleach, Kodak reversal bleach R-9. An argon ion laser with a total intensity near 1.45 μW/cm^2 in the recording plane at a wave length of 514.5 nm was used to expose the plane wave gratings. The interbeam ratio of light intensities (K̆-ratio) was 1.06, and a spatial frequency of 1,000 c/mm was used. Sixty plane wave gratings were prepared on five Kodak 649F plates. A peak diffraction efficiency of 25 percent was observed near an exposure of 200 μJ/cm^2. The spread in data points is seen to increase at the higher exposures. The data point spread is not seen in data taken from a single plate, but only becomes apparent when comparing data points from two or more plates. The angular band width was measured for different exposures and found to be 3 degrees FWHM for each grating.

In figure 18, the effect is shown of changing the K-ratio on the characteristic exposure curve. Not only does the peak diffraction efficiency decrease at the higher K-ratios, but the exposure required to produce a peak efficiency increases for higher K-ratios through K = 10.

In figure 19, the effect is shown of recording at spatial frequencies of 1,000 c/mm and 1,500 c/mm. Since there is very little difference between diffraction efficiencies for the two different spatial frequencies, we expect the SHG process will be shown to be suitable for recording phase volume holograms at spatial frequencies between 500 and 2,000 c/mm.

In figure 20, the efficiency is shown of the SHG process as a function of the pH used in the acid wash and two different rinse baths. With the acid wash a peak efficiency of 0.1 percent was obtained at a pH less than 2.0, indicating that at this pH the Cr^{+3} is removed from the emulsion and that very little crosslinking occurs. The efficiency rapidly increases between a pH of 3.8 and 4.7, but is observed to decrease at the pH of tap water at 7.4. A higher efficiency is observed for the plane wave gratings prepared with a simple acid rinse. A peak efficiency is indicated between a pH of 6.0 and 7.0. An efficiency of 33.5 is seen at a pH of 5.9. Again the diffraction efficiency is observed to decrease for tap water at a pH of 7.5 for the acid rinse. The buffer rinse produces an increase in efficiency, but at a reduced rate than that for the acid rinse. At a pH of 5.1, the efficiency is seen to drop. Apparently there is an interaction between the Cr^{+3} and the acetate radical of the buffer that reduces the amount of crosslinking that occurs in the gelatin molecule.

FIGURE 17.   Silver Halide (Sensitized) Gelatin

λ = 514.5 nm
Spatial Freq = 1000 c/mm
k–Ratio = 1.06
Recording Power = 1.45 mW/cm²
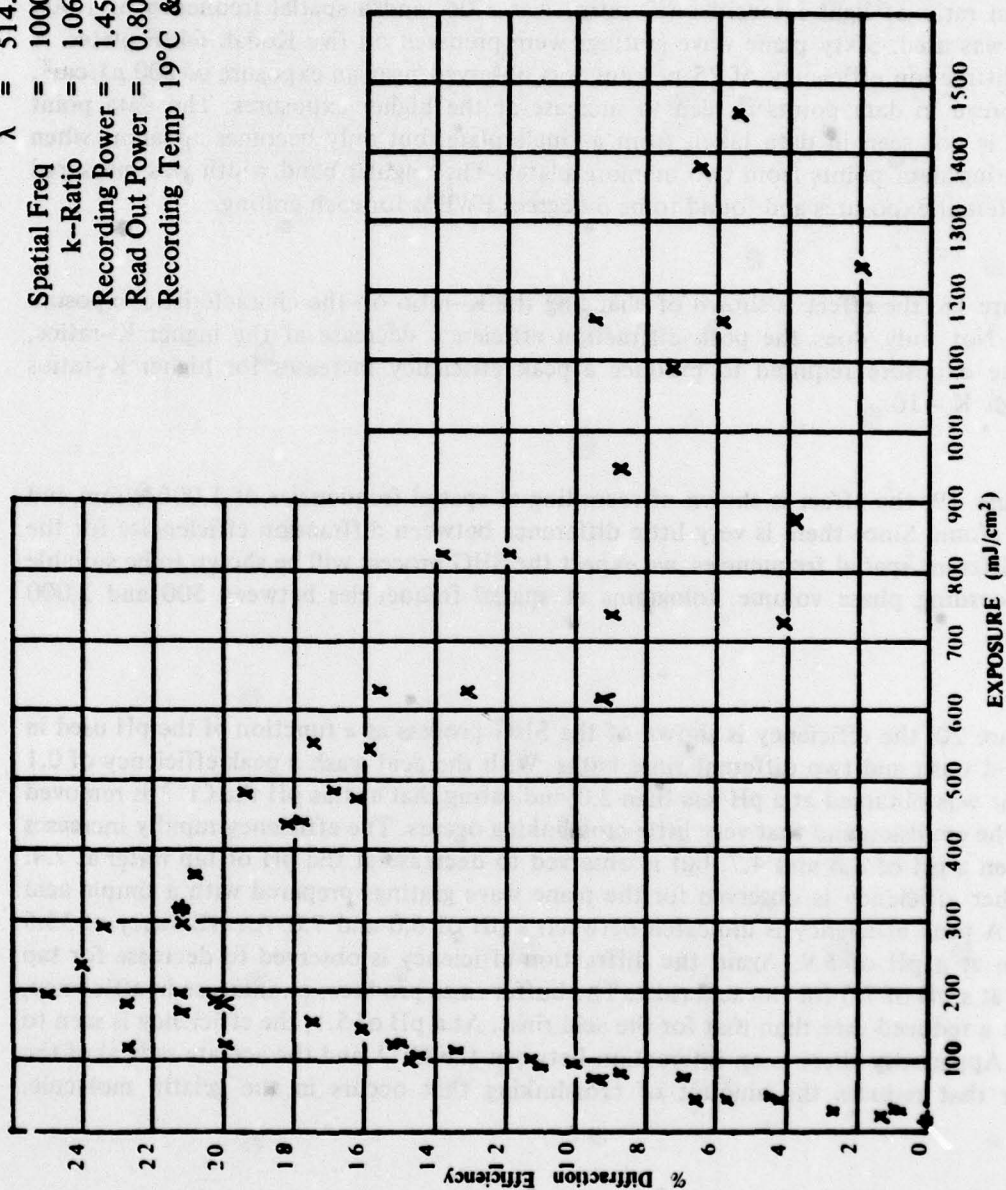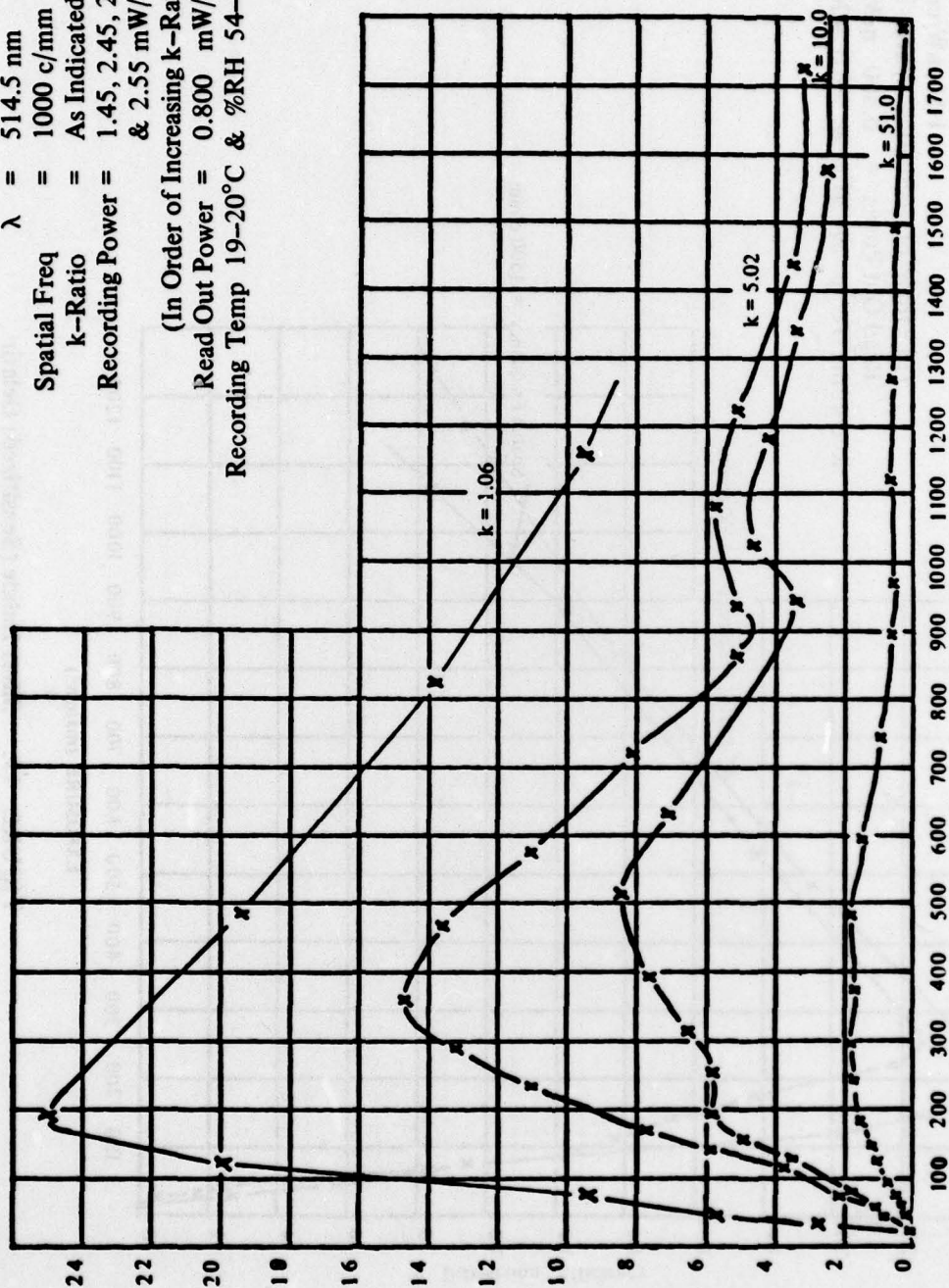Read Out Power = 0.800 mW/cm²
Recording Temp 19°C & %RH 40%

FIGURE 18. Silver Halide (Sensitized) Gelatin

FIGURE 19. Silver Halide (Sensitized) Gelatin

58

% Diffraction Efficiency

Acid
Rinse

Buffer
Rinse

Acid
Wash

λ = 514.5 nm
Spatial Frequency = 1500 c/mm
k - Ratio = 1.00

32
30
28
26
24
22
20
18
16
14
12
10
8
6
4
2
0

1 2 3 4 5 6 7 8 9 10 11
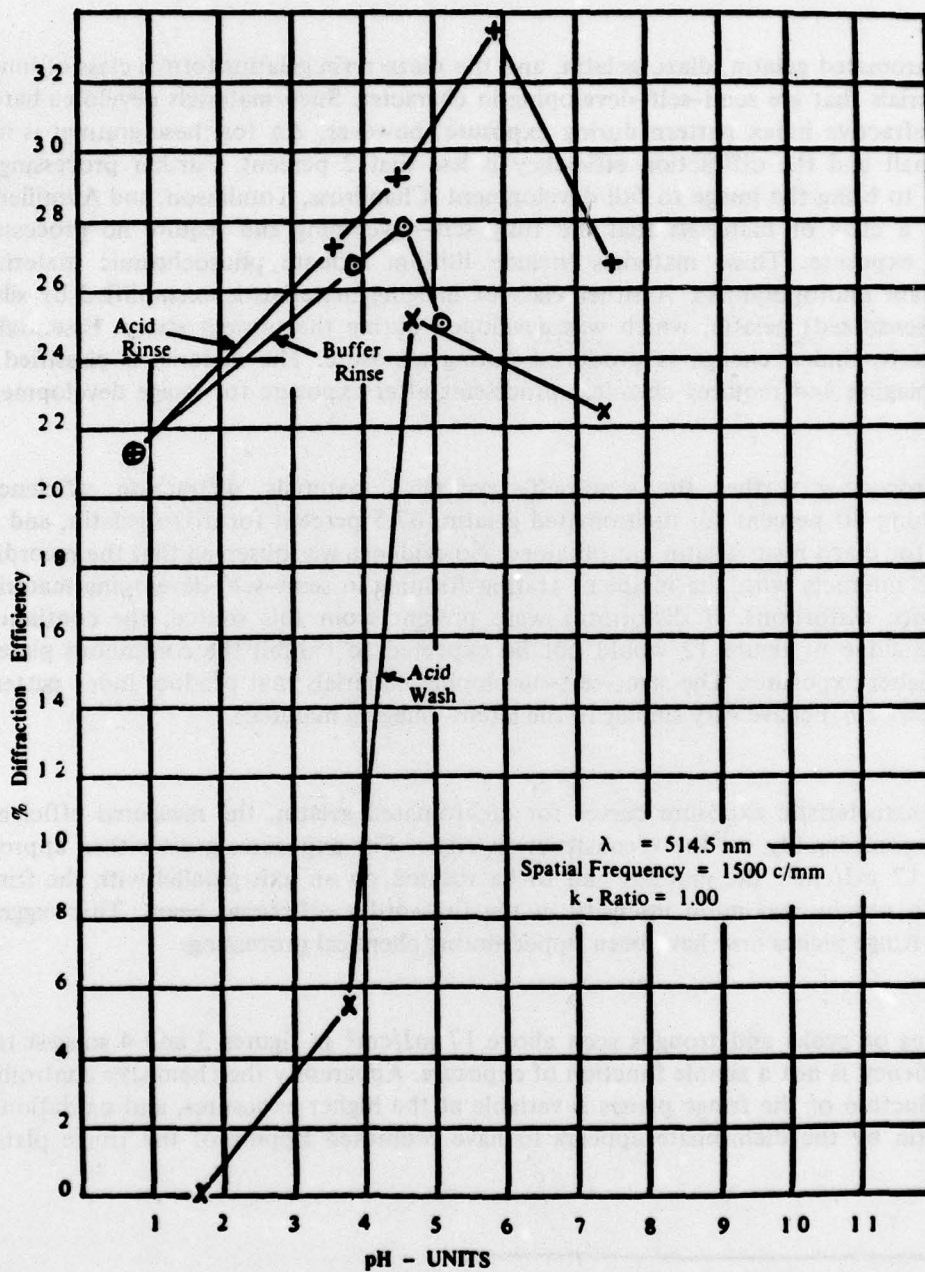
pH – UNITS

FIGURE 20.   Silver Halide (Sensitized) Gelatin

DISCUSSION

The dichromated gelatin, diazo gelatin, and the diazo resin gelatins form a class of imaging materials that are semi–self–developing in character. Such materials develop a barely visible refractive index pattern during exposure; however, $\Delta\eta$ for these gratings is initially small and the diffraction efficiency is less that 2 percent. Further processing is required to bring the image to full development. Chandross, Tomlinson, and Aumiller[23] describe a class of materials that are fully self–developing and require no processing beyond exposure. These materials include lithium niobate, photochromic materials, and certain photopolymers. Another class of imaging materials is exemplified by silver halide (sensitized) gelatin, which was developed during the present study. Essentially, no refractive index change is produced during exposure. The material is classified as latent–imaging and requires chemical processing after exposure for image development.

After processing further the semi–self–developing materials, diffraction efficiencies approaching 80 percent for dichromated gelatin, 67.5 percent for diazo gelatin, and 15 percent for diazo resin gelatin are obtained. No evidence was observed that the recording exposure interacts with the incipient grating forming in semi–self–developing materials to produce distortions. If distortions were present from this source, the continuous exposure curve of figure 12 would not be expected to exhibit the continuous plateau at the higher exposures. The semi–self–developing materials that produce index patterns with a low $\Delta\eta$ behave very similar to the latent–imaging materials.

In the characteristic exposure curves for dichromated gelatin, the measured efficiency depends considerably on the reconstruction angle. For exposures greater than approximately 17 mJ/cm^2, the gratings had to be rotated on an axis parallel with the fringe planes to obtain maximum intensity in the first–order diffracted beam. This suggests that the fringe planes may have been tipped during chemical processing.

The series of peaks and troughs seen above 17 mJ/cm^2 in figures 3 and 4 suggest that the efficiency is not a simple function of exposure. Apparently the chemistry controlling the production of the fringe planes is variable at the higher exposures, and oxidation of the gelatin by the dichromate appears to have promoted tipping of the fringe planes.

---

[23]E. A. Chandross, W. J. Tomlinson, & G. D. Aumiller, "Latent--Imaging Photopolymer Systems," *Applied Optics*, Vol. 17, No. 4., 15 February 1978, p 566.

At exposures below 17 mJ/cm^2, a peak is observed with a maximum efficiency of 70 percent shown in figure 3. Compared to figure 4, there is a drop of 10 percent that appears related to deterioration of the grating in the ambient. In the exposure range below 17 mJ/cm^2, no tipping of the fringe planes is observed.

The process by which refractive index patterns are formed in diazo materials appears complex and not well–defined. A correspondence in diffractive properties between the incipient and the fully processed gratings was observed by monitoring the diffraction of the developing gratings with the He–Ne laser during simultaneous exposure with the Ar$^+$ laser. This suggests that the final measured diffraction depends on the extent to which the individual refractive index patterns are formed initially.

The 7 to 10 identical exposures with diazo gelatin (figure 9) produce widely varying efficiencies and appear independent of exposure. The formation of the refractive index pattern in diazo resin gelatin appears even more unpredicatable than that for diazo gelatin. The statistical data of figure 15 show an even greater variance in efficiency obtained for 10 indentical exposures.

With a few exceptions, diffraction curves reported in the literature for phase volume holograms begin with zero initial slope and increase in a parabolic fashion. Some materials exhibit relatively low efficiencies and saturation behavior. At times, instead of saturation an oscillatory diffraction efficiency is observed. Magnusson and Gaylord[24] have applied a dynamic theory that explains much of the experimental data in the literature. However, their theory would not seem to predict the peaks and troughs we have observed for the diazo and diazo resin gelatins.

The true nature of the diazo materials may have been postulated by Materazzi as a result of his work with the diazo resin for lithographic plate coatings.[25] Materazzi found that instead of the expected linear relationship between the exposure and the amount of

[24] R. Magnusson and T. K. Gaylord, "Use of Dynamic Theory to Describe Experimental Results From Volume Holography," *J. of Applied Physics*, Vol. 47, No. 1, January 1976, p 190.

[25] Albert Materazzi, *Technical Association of the Graphic Arts Proceedings*, 1967, p 229.

lacquer deposited from a wipe on plate developer, there were oscillations in the curve when the weight of lacquer deposited was plotted versus exposure. From these results, he concluded that photolysis of the diazo resin coated on a suitable support does not proceed in a uniform manner and that, perhaps, different species of polymers are produced at different levels of exposure with a varying affinity for the resin in the developer. In the case of our results with the diazo sensitized gelatin, a variety of polymers might be formed with varying degrees of ability to tan the gelatin. This in turn would result in oscillatory patterns of efficiency with exposure.

Phase volume holograms have been produced using several photosensitive processes. Two classes of processes are of particular interest as they can be used to demonstrate advantages of the silver halide (sensitized) gelatin process. One class are the bleached silver halide processes and the second class is the hardened dichromated gelatin process. In the bleached silver halide processes, a high resolution, panchromatic silver halide film or plate (e. g. Kodak 649F plate) is used. Exposures on the order of a few tenths (0.2 to 0.3) of milliJoules per square centimeter (mJ/cm^2) are used at any wavelength in the visible light spectrum. After exposure, the plate is developed and fixed, followed by direct bleaching of the remaining silver metal with one of a number of bleaching agents. In this case, the phase volume hologram formed consists of silver halide in a gelatin matrix. The refractive index difference between the silver halide and the gelatin produces the hologram. The primary difficulties with the bleached silver halide holograms are noise and printout effects. Printout occurs when silver halide is slowly reduced to silver metal by actinic light. Hardened dichromated gelatin exhibits minimal light scatter or noise and no printout phenomena. The hardened dichromated gelatin plates are usually prepared as outlined earlier in this report. Exposures on the order of ten to a few hundreds (10 to 300) of mJ/cm^2 are required at wavelengths below 515 nanometers (nm). After processing, the phase volume hologram formed consists of crosslinked or tanned gelatin in a gelatin matrix. The primary difficulties with the hardened dichromated gelatin process are the high exposure requirement, the limited spectral response (e.g. $\lambda \leqslant 515$), and the lack of storage ability of the sensitized dichromated gelatin emulsion.

The SHG process provides advantages of both bleached silver halide processes and the hardened dichromated gelatin process without their distinct disadvantages. In the SHG process, a high resolution, panchromatic silver halide film or plate (e.g. Kodak 649F) is used. Following exposure, the plate is processed as described earlier. The basic chemistry of the process appears to be the formation of the Cr^{+3} in the Kodak R-9 bleach by the following reaction:

$$6Ag^\circ + Cr_2O_7^= + 14H^+ \longrightarrow 6Ag^+ + 2Cr^{+3} \quad 7H_2O$$
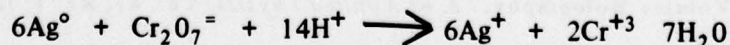
The Cr^{+3} then presumably crosslinks the gelatin in the immediate vicinity of the silver metal image. The experiments with the wash and two different rinse baths in which the pH of the baths was adjusted suggests that the Cr^{+3} does not permanently crosslink the gelatin molecule until the emulsion is removed from the Kodak R–9 bleach bath and is placed in the appropriate bath with a higher pH (e.g. a pH of between 6 and 7 for the acid rinse as shown in figure 20). The completely processed phase volume hologram that is formed consists of crosslinked gelatin in a gelatin matrix that is perhaps similar to that obtained in the hardened dichromated gelatin process. Thus, the SHG process possesses the low exposure requirements, spectral sensitivity, and shelf–life characteristic of the silver halide processes and possesses the low noise and absence of printout characteristic of dichromated gelatin.

The efficiency versus exposure curves for the SHG process suggest that the formation of the refractive index pattern is a well–behaved function of the exposure. In figure 18 a progressive and uniform change in the efficiency is illustrated for each incremental change in exposure. The variance in efficiency at exposures greater that $200 \ \mu J/cm^2$ in figure 17 suggests that the SHG process may be sensitive to certain variables, such as the rate of agitation, temperature, and percent relative humidity, or minute differences in processing times. Still the variance in efficiency is seen to be small at exposures less than $200 \ \mu J/cm^2$, which may be the working portion of the characteristic exposure curve. Further, the SHG process produces its refractive index pattern through a latent image. Thus, there is no possibility of the exposing light interacting with a self–developing grating to produce distortions in the holographic fringe planes. The SHG gelatin process appears to be a new and unique method for making phase volume holograms.

In March 1979, a patent was filed with the U. S. Patent and Trademark Office.[26] This application treats the SHG process.

---

[26] Patent Application Number 23,217, "Process for Making Phase Holograms," 23 March 1979.

63

CONCLUSIONS

1.   The literature reviewed during the course of this work indicates that self–developing materials produce refractive index patterns during exposure with sufficiently large $\Delta\eta$ to cause interactions between the patterns and the recording beam. This interaction causes distortions in the recorded image.

2.   Semi–self–developing materials such as dichromated, diazo, and diazo resin gelatins also develop refractive index patterns during exposure, but with much smaller $\Delta\eta$. These patterns produce very little scattering of the recording beam, and no appreciable distortion in the recorded image was detected from this source by our methods.

3.   The latent–imaging materials such as the silver halide (sensitized) gelatin produce no changes in refractive index during exposure. There are no changes in the optical properties of the material, and therefore there are no distortions introduced in the recorded image during exposure.

4.   Diffraction in dichromated gelatin appears to be a function of exposure below about 17 mJ/cm^2 at 488.0 nm recording wavelength. At higher exposures the gelatin appears to be oxidized by the photolyzed dichromate with the result that the diffraction efficiency is unpredictable.

5.   In diazo and diazo resin gelatin, the formation of the refractive index patterns is apparently a complex process that produces unpredictable results.

6.   Silver halide (sensitized) gelatin is a latent–imaging material that produces refraction index patterns whose efficiencies are a predictable function of exposure.

7.   Of the four processes studies, silver halide (sensitized) gelatin offers the most promising potential. This process has a broad spectral response, low exposure requirements, and a good shelf–life compared to dichromated gelatin. The SHG process does not suffer from the printout phenomena characteristic of the bleached holographic recording materials.

8.   The unpredictable results obtained with diazo and diazo resin gelatin preclude their use as holographic recording materials. However, further knowledge of the chemistry of these materials might lead to a better understanding of tanning processes in gelatin.

FUTURE STUDIES

Of the four processes described in this report, silver halide (sensitized) gelatin appears to offer the greatest potential for development into a usable holographic recording material with favorable process characteristics. This process warrants more study. An effort should be made to further increase the efficiency, signal–to–noise ratio (SNR), and the geometric fidelity with which the reconstructed image is formed. Process improvements can be sought in further studies of the effect of pH of processing baths, the use of heated isopropanol in the dehydrating step, and the use of an oven in the drying step. Studies of diffraction efficiency, SNR, and geometric fidelity at various temperatures and RH's should be conducted with the environmental test facility currently being constructed. These studies are essential to understanding whether or not a particular holographic recording material will have archival properties and be free of distortions in the reconstructed image.